Naval Research Laboratory

Washington, DC 20375-5320

NRL/MR/6120--11-9368

Report on Scientific Basis for Paint Stripping: Mechanism of Methylene Chloride Based Paint Removers

JAMES H. WYNNE

Materials Chemistry Branch
Chemistry Division

KELLY E. WATSON

SAIC
Washington, D.C.

JAMES P. YESINOWSKI

Materials Chemistry Branch
Chemistry Division

CHRISTOPHER N. YOUNG
CLIVE R. CLAYTON

Stony Brook University
Stony Brook, New York

NICK NESTERUK
JACK KELLEY
TOM BRASWELL

U.S. Army Research Laboratory
Aberdeen Proving Ground, Maryland

October 20, 2011

REPORT DOCUMENTATION PAGE

Form Approved
OMB No. 0704-0188

1. REPORT DATE *(DD-MM-YYYY)*	**2. REPORT TYPE**	**3. DATES COVERED** *(From - To)*
20-10-2011	Memorandum Report	01 May 2009 - 31 Aug 2011

4. TITLE AND SUBTITLE

Report on Scientific Basis for Paint Stripping: Mechanism of Methylene Chloride Based Paint Removers

5a. CONTRACT NUMBER

5b. GRANT NUMBER
61-9512-F0-5

5c. PROGRAM ELEMENT NUMBER

6. AUTHOR(S)

James H. Wynne, Kelly E. Watson,* James P. Yesinowski, Christopher N. Young,†
Clive R. Clayton,† Nick Nesteruk,‡ Jack Kelley,‡ and Tom Braswell‡

5d. PROJECT NUMBER

5e. TASK NUMBER

5f. WORK UNIT NUMBER

7. PERFORMING ORGANIZATION NAME(S) AND ADDRESS(ES)

Naval Research Laboratory
4555 Overlook Avenue, SW
Washington, DC 20375-5320

8. PERFORMING ORGANIZATION REPORT NUMBER

NRL/MR/6120--11-9368

9. SPONSORING / MONITORING AGENCY NAME(S) AND ADDRESS(ES)

Strategic Environment Research and Development Program
901 North Stuart Street, Suite 303
Arlington, VA 22203-1853

10. SPONSOR / MONITOR'S ACRONYM(S)

SERDP

11. SPONSOR / MONITOR'S REPORT NUMBER(S)

WP-1682

12. DISTRIBUTION / AVAILABILITY STATEMENT

Approved for public release; distribution is unlimited.

13. SUPPLEMENTARY NOTES

*Science Applications International Corporation (SAIC), 4555 Overlook Ave, SW, Bldg. 207, Room 302, Washington, DC 20375-5320
†Stony Brook University, Dept. of Materials Science and Engineering, 2275 SUNY Engineering Bldg. 314, Stony Brook, NY 11794
‡U.S. Army Research Laboratory, B4600 Deer Creek Loop, Aberdeen Proving Ground, MD 21005

14. ABSTRACT

Chemical paint strippers that include methylene chloride and phenol have been extensively used to remove coatings from metallic substrates. These strippers are inexpensive and remove polymeric organic coatings quickly and easily from a variety of metallic substrates without damage to the substrate. Their mechanism of action has not been adequately characterized. Herein we report changes in physical and molecular-level properties of five coatings upon exposure to components of the paint stripper including methylene chloride and phenol. The coatings studied were polyurethane topcoats and epoxy primers currently in military use, both clear films and fully pigmented films. The development and use of simplified formulations (clear films) of each coating was done. The coatings were characterized using DSC, TGA, solid state ^{1}H- and ^{2}H-NMR spectroscopy, Raman spectroscopy, X-ray photoelectron spectroscopy and attenuated total reflectance FTIR. Our results show very different behavior for methylene chloride and phenol. Methylene chloride acts by penetrating the coating and enabling other solvents in penetrating the coating. These other solvents, in particular water and phenol, are responsible for coating degradation.

15. SUBJECT TERMS

Paint stripper
Methylene chloride
Phenol
Polyurethane

16. SECURITY CLASSIFICATION OF:			**17. LIMITATION OF ABSTRACT**	**18. NUMBER OF PAGES**	**19a. NAME OF RESPONSIBLE PERSON**
					James H. Wynne
a. REPORT	**b. ABSTRACT**	**c. THIS PAGE**	UU	72	**19b. TELEPHONE NUMBER** *(include area code)*
Unclassified	Unclassified	Unclassified			(202) 404-4010

Standard Form 298 (Rev. 8-98)
Prescribed by ANSI Std. Z39.18

This page intentionally left blank.

Table of Contents

List of Figures

List of Tables

Report on Scientific Basis for Paint Stripping: Mechanism of Methylene Chloride Based Paint Removers

Abstract

Chemical paint strippers that include methylene chloride and phenol have been extensively used to remove polymer coatings from metallic substrates. These strippers are inexpensive and remove polymeric organic coatings quickly and easily from a variety of metallic substrates without damage to the substrate. However, due to environmental and health concerns there is increasing pressure to replace methylene chloride with less hazardous alternatives. Although various alternatives to these organic solvent based systems have been developed, none equal their effectiveness in performance or cost. Thus far the mechanism of action of chemical strippers has not been adequately characterized. In order to experimentally determine the paint removal mechanisms of methylene chloride, it was important to first limit the variables in the overall process. Many of the more prominent variables exist in the coating itself, and therefore the development of simplified formulations (clear films) of each coating of interest is a logical direction. Herein we report changes in physical and molecular-level properties of five polymer coatings upon exposure to components of the paint stripper including methylene chloride and phenol. The coatings studied were polyurethane topcoats and epoxy primers currently in military use. Using proprietary information supplied by a paint supplier, we combined the resin binders and curing agents as specified to attempt to produce clear coat films. Initial attempts failed because it was learned that the pigments and extenders provided beneficial effects in the curing process. To compensate for this, significant modifications to the original formula were necessary to affect flow characteristics in order to facilitate the creation of a continuous smooth film.

Changes to the physical and molecular-level properties of the coatings upon exposure to components of the paint stripper were characterized using differential scanning calorimetry (DSC), thermogravimetric analysis (TGA), gas chromatography with mass spectrometry detection (GCMS), solid-state proton (^{1}H) and deuterium (^{2}H) nuclear magnetic resonance spectroscopy (NMR), Raman spectroscopy, X-ray photoelectron spectroscopy (XPS), and attenuated total reflectance Fourier transform infrared spectroscopy (FTIR-ATR). Our results show very different behavior for methylene chloride and phenol. Methylene chloride acts as a good solvent, penetrating the coating and acting as a facilitator for the other solvents in penetrating the coating. NMR results show that methylene chloride solvates the polyurethane topcoat coating and is in close contact with the polymer chains. FTIR-ATR results show dilation

Manuscript approved September 15, 2011.

of the carbonyl bond of the polyurethane backbone which would allow for easier diffusion of larger solvent molecules into the coating. However, DSC shows that exposure to methylene chloride alone does not degrade the coating. Our results of solutions containing solvents, in particular water and phenol, which are only able to penetrate the coatings due to the presence of methylene chloride, do show coating degradation. FTIR-ATR and XPS results indicate a hydrolysis reaction occurring in localized regions of the coatings exposed to methylene chloride/ethanol/water solutions. The thermal data show exposure to phenol containing solutions to cause the most coating degradation. ^{1}H NMR data suggest that the solvents in the paint stripper rapidly exert very significant effects that increase the polymer segmental dynamics in a fashion similar to what takes place in the untreated coatings by heating them to much higher temperatures. FTIR-ATR analysis shows phenol within exposed samples well after drying, indicating the molecule is bound to the polymer resin either by chemical reaction or steric hindrance. Deuterium NMR of d_2-MC (CD_2Cl_2) at various temperatures shows that the methylene chloride molecule present in a polyurethane topcoat is not rigid but rather undergoes isotropic rotational tumbling. The rate of tumbling however is orders of magnitude slower than that in solvents, suggestive of weak interactions with groups on the polymer, perhaps via electric dipoles. The deuterium NMR of an epoxy primer exposed to d_5-phenol/ethanol for different lengths of time reveals a wealth of detailed dynamical information for each sample exposure from changes in the spectral appearance and the T_2 as a function of temperature. Molecular dynamics behavior ranging from rigid phenyl rings on the phenol, to 180º ring flips, to anisotropic motions of varying amplitudes, to completely isotropic motions, are observed. The results suggest a model in which phenol inserts itself into the polymer backbone via nucleophilic attack that could be responsible for this inflexibility. A color change was observed in phenol exposed coatings which could be due to the increased conjugation caused by phenol's incorporation into the polymer. The most reactive mixture of methylene chloride/ethanol/water/phenol causes sample degradation to such an extent that most samples are too degraded to allow for analysis. Nucleophilic attack of the polymer backbone by phenol is suggested by these data but confirmation of this specific reaction pathway has been difficult to achieve.

Objective

The objective of this project is to monitor the changes in physical and molecular-level properties of polymeric coatings after exposure to the components of organic solvent based paint strippers and by doing so to determine the mechanism by which organic solvent based paint strippers remove polymeric coatings from their substrate, specifically to determine the roles that methylene chloride and phenol play in the coating's removal.

Background

Historically, chemical paint strippers based on methylene chloride and phenol were widely used to remove polymeric coatings. These strippers were highly effective, inexpensive and exhibited minimal impact on the substrate. However, environmental and health concerns suggest the need for replacements. Replacement attempts have led to more environmentally friendly alternatives at the cost of performance, price, and substrate damage.[1] The mechanism by which methylene chloride and phenol work to remove polymeric coatings has not been fully characterized,[2] despite over 50 years of research in this area[3]. One major avenue of investigation has been to analyze physical changes in relation to adhesion loss. The conclusion of this research has been that solvent-based paint removing formulations wet the paint surface and then penetrate the layers to the substrate by diffusion through the coating.[4, 5] It is thought that the small molar volume solvents, *i.e.* water and methylene chloride, are able to penetrate the coating by more easily "fitting" into spaces between the polymer molecules and diffusing through these spaces and channels.[6] Polarity and other physical properties of the solvent also play a strong role in the ability to solvate the coating. The physical changes to the coating, such as swelling, cause adhesion loss by disrupting the polymer layers and breaking hydrogen bonds or other intermolecular forces. Generally, swelling reduces the stress necessary to fracture the coating by increasing the strain on the polymer network. Experimentally this is seen by the ease of scraping off a solvated coating versus a dry coating from a substrate. There has been some investigation into the chemical interactions between solvents and the coating,[7] including evidence of the influence solvents have on the polymer structure.

To effectively elucidate the effect of chemical paint stripper on polymeric coatings, some well characterized control polymeric coatings are needed. Commercial coatings contain not only the binder but also various pigments, fillers, flattening compounds, pigment related dispersion and wetting agents. To reduce complications, some of this work employed control coatings made without these components. The clear films were made of five military specified coatings including three epoxy primers (MIL SPEC: 85582, 23377, and 53022) and two polyurethane topcoats (MIL SPEC: 53039 and 85285). Films of the same military specified coatings in their full formulation were also studied. As a final control limited studies were performed on partial

formulations of the specified coatings, that is, formulations containing all of the full formulation components except the flattening agents.

This work aims to use wet organic chemistry, solid-state proton and deuterium NMR spectroscopy, thermal analysis and vibrational spectroscopy to understand the mechanism of how methylene chloride based paint removers remove polymeric coatings and so fill the knowledge gap in this area.

NMR Spectroscopy Strategy

In terms of deciding upon a strategy for using NMR spectroscopy, three nuclei were considered that represented feasible candidates for NMR study: ^{1}H, ^{2}H, and ^{13}C. For alkyd paint binders swollen overnight by deuterochloroform, it was shown that reasonably high-resolution ^{13}C spectra were obtainable using a conventional liquid-state NMR spectrometer.[8] However, for the initial stages of solvent penetration such an approach would not succeed because the reduced mobility of the polymer chains would give more solid-like ^{13}C spectra requiring techniques such as cross-polarization (CP) and magic-angle spinning (MAS). These techniques have indeed been applied to monitor dynamics in water- or acetone-swollen ionizable polymer networks by monitoring ^{13}C relaxation times;[9] a number of ^{13}C and ^{1}H NMR studies have been reported on swollen polymer networks, but not in paint coating systems.[1011,12,13] Although initial experiments yielded a ^{13}C CP-MAS NMR spectrum of a polyurethane topcoat film (data not shown), it was decided to concentrate on static (stationary) rather than MAS for NMR because of the problems anticipated with the large centrifugal forces in the case of spinning samples that would tend to expel the solvent from the polymer film and make spinning difficult as well. Static ^{1}H solid-state NMR is also a very convenient and sensitive way of monitoring the increase in segmental dynamics upon swelling. In terms of observing NMR of the solvent molecules themselves, ^{1}H NMR can be useful in more highly swollen cases such as chloroform in copolymer gel beads,[14] or in diffusion studies of organic solvents in polyisoprene.[15] However, labeling the solvent with deuterium provides greater selectivity (because of the low natural-abundance of ^{2}H, 0.015%) as well as greater sensitivity to and theoretical interpretability of molecular dynamics and orientation due to the dominance of the large nuclear quadrupole interaction. This is exemplified by ^{2}H NMR studies of D_2O in epoxy[16] and nylon[17] and deuterated small organic molecules used to probe stress/strain effects in polymers[18,19] including

d_5-phenol in nylon.[20] We found that in our systems solid-state ^{2}H NMR reveals a wealth of detailed dynamical information from changes in the spectral appearance and the T_2 as a function of temperature. In particular, we observe marked reductions in the rate of molecular tumbling (i.e. increases in the rotational correlation times) for solvent molecules in the polymer matrix, compared to in solution, especially for lower degrees of swelling. Molecular tumbling of solvent molecules or nitroxide spin probes covalently attached to polymer backbones has previously been studied by EPR spectroscopy[21-25] as well as ^{13}C NMR[10] and similar conclusions were obtained.

Solid-state proton (^{1}H) NMR shows the effects of exposure to the control solvent mixtures on the segmental dynamics of the polymer chains. It also affords insight into the physical state of the solvent molecules of methylene chloride by indicating that the molecules are primarily in atomic-level contact with polymer molecules rather than in a larger pool of other solvent molecules. The changes as a function of temperature in the spin-lattice relaxation times (T_1), the spin-lattice relaxation times in the rotating frame ($T_{1\rho}$), and the spectra's peak widths at half-height (HHLW) after exposure to methylene chloride or phenol/water solutions are reported. Studies were done as a function of temperature to allow for comparison between dynamics induced from solvent exposure and those induced solely by increase in temperature.

Thermal Analysis Strategy

Thermal analysis of the coatings before and after exposure to control solvent mixtures of individual components typically found in commercial paint stripper can give insight into the degradation caused by the paint stripper. By studying the change in glass transition temperature, T_g, the specific solvent mixtures that were responsible for significant degradation of the coatings were identified. Differential Scanning Calorimetry (DSC) scans taken of coatings after exposure to the control solvent mixtures show decreases of the glass transition temperature by as much as 100 °C. Changes in the Thermogravimetric Analysis (TGA) curve can also illustrate a solvent mixture's activity and suggest both the physical and chemical degradation mechanism.

Vibrational Spectroscopy and XPS Strategy

Spectroscopic analysis of military coating systems can be hampered significantly by the presence of fillers and pigments. Raman spectroscopy is a visible light technique, wherein pigments

dominate the resulting spectrum, while polymeric fillers overlap significantly with the small amount of binder present in a given sample spot. While the effect is not as pronounced when studying samples with FTIR or XPS methods, the significant contribution of these components compared to the binder makes analysis of the latter quite difficult. In order to overcome this problem, clear versions of each coating were required. Later, partially-formulated coatings can be studied once the changes to the binder have been understood.

It was hoped that studying the coatings before and after solvent exposure, would provide insight into any chemical changes. However, in some cases the solvent dried out of the sample and left the exposed coating in a very similar state to the unexposed coating. Use of the Raman spectrometer enables the study of the sample while it is saturated with solvent, which has led to some interesting results.

The FTIR method employed here was attenuated total reflectance (ATR), which analyzes the top few microns of a sample. Through this experiment significant surface effects as a result of exposure were observed. In order to better understand these changes, X-ray photoelectron spectroscopy (XPS) was employed, which provides spectral information of the top few nanometers.

Comparison of the spectra of the coatings saturated with solvent or after exposure to solvent with those of unexposed coatings suggested changes in the coating's structure and thus aided in the mechanistic elucidation.

Materials and Methods

Chemicals

All chemicals were reagent grade and used without further purification. Mixtures were prepared by weight according to ratios listed in Table 1.

Table 1. List of the composition of the control solvent formulations.

		Weight Percent			
		methylene chloride	ethanol	water	phenol
Solution	Commercial paint stripper[a]	60.6	5.8	7.8	15.8
	Methylene chloride	100	---	---	---
	Methylene chloride and ethanol	91	9	---	---
	Methylene chloride, ethanol and water[b]	82	8	10	---
	Methylene chloride, ethanol, water and phenol[b]	67	6	9	18
	Phenol and methylene chloride	79	---	---	21
	Phenol and ethanol	---	27	---	73

[a]Also contains Methocel (1.2%), toluene (1.3%), sodium petroleum sulfonate (5.5%) and paraffin wax (1.9%),
[b]Methocel added to emulsify into a single phase.

Coatings

Currently employed military coatings were selected for this study. These included two polyurethane topcoats and three epoxy primers. The coatings were unsupported (free films) with a film thickness of approximately five mils, see Table 2, of five military coatings; MIL-PRF-23377, MIL-PRF-85582, MIL-DTL-53039, MIL-PRF-85285, and MIL-PRF-53022.

Table 2. Current military coatings studied.

Military Specification	Finial thickness clear (mm)	Final Thickness partially formulated (mm)	Final Thickness fully formulated (mm)	Specific coating description
MIL-DTL-53039	0.13	0.06	0.14	Single Component Aliphatic Polyurethane CARC Topcoat
MIL-PRF-85285	0.13	0.07	0.20	Two Component High Solids 2.8 VOC Polyurethane Topcoat
MIL-PRF-23377	0.13	na	0.17	Two component Chromated Epoxy Polyamide Primer
MIL-PRF-85582	0.17	na	0.15	One component Waterborne Chromated Epoxy Primer
MIL-PRF-53022	0.12	na	0.16	Lead and Chromate Free Epoxy Primer

Complete coating formulations can be found in Tables 3-6. The simplification of the otherwise complex coating system was selected to allow for ease of analysis. Resin binders and curing agents were combined as specified in Tables 7-10 to produce clear coat films of the selected four military coatings. Each clear coat formulation was produced without pigments, additives, and solvents. In order to cast clear formulations to the required film thickness it was necessary to compound formulas to a workable spray application viscosity by adding the solvents contained in each formula in the proportions and thinning ratios specified. Elimination of entrapped air or

solvents required either the addition of an antifoam agent or the readjustment of antifoam agent amounts or both. Antifoam agents used were those normally contained in each formula and were added in the proportions specified in Tables 7-10.

Complete Coating Formulations:

Table 3. MIL-PRF-23377 Epoxy Polyamide Primer.

Part A Raw Material	Wt %	**Part B** Raw Material	Wt %
Acetone	12	Acetone	0.7
2,4,6-Tri(dimethylaminomethyl) phenol	0.5	Methyl *N*-amyl ketone	1
Fatty aminoamide	1	Dimethyl glutrate & succinate	1.2
Butyl urea formaldehyde	2.2	Epoxy resin	14.7
Polyamid resin	7		
Dispersion agent	0.2		
Silica gel	3		
Ceramic microspheres	3		
Titanium dioxide	6.5		
Extender pigment	47		

Table 4. MIL-DTL-53039 Single Component Aliphatic Polyurethane CARC.

Raw Material	Wt %	Raw Material	Wt %
Polyurethane	31	Cobalt titanate spinel	0.4
Dispersant	1	Methyl isoamyl ketone	23.5
Rheology modifier	0.1	VM&P naptha	3.2
Flow modifier	<0.1	Xylene	1.4
Surfactant	0.1	*n*-Butyl acetate	1.3
Dibutyl tin dilaurate	0.5	Aromatic 100	1.3
Celite	18.5	Mineral spirits	1.2
Imsil	3.6	Propylene glycol	0.1
TiO_2	9.5	Isobutyl ketone	0.1
Iron oxide hydrate	2.5	*n*-Butyl acid phosphate	0.1
Carbazole dioxazine violet	<0.1	Bentone	0.5

Table 5. MIL-PRF-85285 High Solids Polyurethane Topcoat.

Part A Raw Material	Wt %	**Part B** Raw Material	Wt %
Methyl *N*-propyl ketone	1	Polyurethane resin	43
Methyl *N*-amyl ketone	7	*N*-Butyl acetate	1.6
Anti-oxidant	0.3		
UV-absorber	0.5		
UV stabilizer	1		
Polyester solution #1	19.3		
Cellosolve acetyl butyrate	0.6		
Surfactant	0.1		
1% Thickener in xylene	0.2		
Thixotropic agent	0.2		
Dispersing agent	0.3		
TiO_2	20.5		
Polyester solution #2	4.4		

Table 6. MIL-PRF-85582 Waterborne Epoxy Primer.

Part A Raw Material	Wt %	**Part B** Raw Material	Wt %
2-Propanol	1.8	Epoxy resin	17
2-Propoxyethanol EP	4	Bisphenol A epichorohydrate	20
Glycol ether DPNB	1	Deionized water	6.8
Acetone	3		
Triaminosilane	1.2		
Non-ionic acrylic copolymer	0.3		
Polyamine curing agent	1.2		
Amine functional emulsion	18.1		
Modified aliphatic amine	1.2		
Natural silica	6		
Silica 10 micron	6		
Magnesium silicate-flakey	2.4		
TiO_2	2.7		
Aqueous carbon black dispersion	<0.1		
Strontium chromate	7.3		

Clearcoat Formulations:

Table 7. MIL-PRF-23377 Epoxy Polyamide Primer Type Clearcoat.

Part A	Wt %	**Part B**	Wt %
Polyamid resin	19.2	Epoxy resin	41.2
Fatty aminoamide	2.8	Methyl *N*-amyl ketone	2.8
Butyl urea formaldehyde	6.2	Acetone	5.9
Acetone	20	Dimethyl glutarate & succinate	1.2
2,4,6-Tri(dimethylaminomethyl) phenol	0.5		
Dispersant	0.2		

Table 8. MIL-DTL-53039 Single Component Aliphatic Polyurethane CARC Clearcoat.

Raw Material	Wt %
Polyurethane	47.4
Dibutyl tin laurate	0.7
Dispersant	0.1
n-Butyl acetate	2
Methyl isoamyl ketone	38.2
Surfactant	0.2
Flow modifier	0.1
Rheology modifier	<0.1
VM&P naptha	4.8
Xylene	2.1
Aromatic 100	2
Mineral spirits	2
Propylene glycol	0.0
Isobutyl ketone	0.2
n-Butyl acid phosphate	0.2

Table 9. MIL-PRF-85285 High Solids Polyurethane Topcoat Type Clearcoat.

Part A Raw Material	Wt %	**Part B** Raw Material	Wt %
Polyester solution #1	24.4	Polyurethane resin	54.4
Polyester solution #2	5.5	*N*-Butyl acetate	2
Methyl *N*-amyl ketone	8.9		
Methyl *N*-propyl ketone	1.3		
Anti-oxidant	0.4		
UV absorber	0.6		
UV Stabilizer	1.3		
Cellosolve acetyl butyrate	0.8		
Surfactant	0.2		
1% Thickener in xylene	0.2		

Table 10. MIL-PRF-85582 Waterborne Epoxy Primer Type Clearcoat.

Part A Raw Material	Wt %	**Part B** Raw Material	Wt %
Amine emulsion	24	Epoxy resin	22.1
Anquamine	1.5	Bisphenol A epichorohydrate	26
Curing agent	1.5	Deionized water	5
2-Propanol	2	Antifoam	1
2-Propoxyethanol EP	5		
Glycol ether DPNB	1		
Acetone	4		
Triaminosilane	1.5		
Non-ionic acrylic copolymer	0.4		

The formulas were compounded to achieve continuous, anomaly-free films of the desired thickness by utilizing the identical rheology and flow modifiers specified in each formula. Clear films were created by spray application after altering the proportions of solvents, adhesion promoters, antifoamers, rheology, and flow modifiers utilized in each clear coating formulation as necessary. Initial application using conventional spray equipment failed due to the high viscosity of the formulations. A drawdown mechanism of application for creating coatings also failed as creating films of the approximate four mils thickness in a single application trapped gas and formed bubbles upon curing. For the material to cure properly to achieve the required film thicknesses, it was necessary to apply multiple film layers, allowing each to cure before applying another layer. This was crucial to avoid solvent entrapment and the resulting complications. All formulations were sprayed in multiple layers on release paper allowing 16-24 hour cure time between each layer and a final seven day cure time. This minimized bubble formation and created coatings of the desired thickness. All clear coatings were prepared on release paper.

Sample Exposure

Thermal analysis samples

For thermal analysis the samples were exposed as follows: Approximately two centimeter square coupons of each coating were cut and placed into individual scintillation vials. To each vial was added the respective solvent or solvent mixture (see Table 1) until the coating was completely covered (~10 mL). After exposure periods of two hours and two days, respectively, the liquid was decanted, rinsed with absolute ethanol and the coating allowed to air dry in the vial. A rinse with ethanol ensured that no remaining chemicals were adhered to the surface of the coating prior to analysis. Caution was taken to ensure the coating was completely dry before testing.

Raman samples

For Raman spectroscopy the samples were exposed to individual solvents or solvent mixtures for times ranging from 15 minutes to two hours. The samples were then air dried thoroughly, for times ranging from two hours to two weeks, to reduce spectral contamination from residual solvent. Solvents systems used included liquid phenol (89:11 phenol/water) as well as a selection of the solvent mixtures listed in Table 1.

NMR samples

The ^{1}H NMR studies were done on MIL-DTL-53039 before and after a five minute room-temperature exposure to methylene chloride and on MIL-PRF-23377 before and after a ten minute room-temperature exposure to a phenol:ethanol (2.724:1 weight ratio) solution. The exposures were performed by immersing squares of the cut film in the solvent in a beaker, removing, and blotting dry before placing into a 5 mm glass NMR tubes loosely sealed with Teflon tape to minimize evaporation.

Samples for ^{2}H NMR were prepared similarly. The MIL-DTL-53039 film was exposed to d_2-methylene chloride (CD_2Cl_2) for 10 minutes at 21º C, and after blotting dry showed a 34.9 wt.% increase in weight (that very slowly dropped on the balance, before being placed in the NMR tube). Two samples of the MIL- PRF-23377 film were prepared with different exposure times to deuterated phenol/ethanol solvent. The d_5-phenol (labelled with 98 atom % D on the aromatic ring) was obtained from Cambridge Isotopes Laboratory and was stored in a brown bottle in a

freezer before use, because of its tendency to decompose slowly. Because of the slightly higher formula weight in the deuterium-substituted phenol, the d_5-phenol/ethanol solvent was prepared with a somewhat higher weight ratio of 3.115:1 than used for the all-proton solvent mixture above. The mole ratio of the two components in the deuterated mixture was very similar (only 8.6% higher) to that in the protonated mixture. One MIL- PRF-23377 sample exposed to the deuterated solvent mixture for 10 minutes at 21º C showed a 21.4 % weight gain. A second sample exposed at 21º C for two hours showed a 124.5% weight gain, with the film crumbling into fragments when handled with tweezers.

Experimental Methods

Differential Scanning Calorimetry (DSC)

Differential scanning calorimetry (DSC) was performed on a TA Instruments Q20 DSC with the DSC Refrigerated Cooling System (RCS) and a purge gas of nitrogen set to 50 mL/min. Samples of approximately 1-2 mg were placed into TA Instrument Tzero Aluminum pans and an empty aluminum pan was used as reference. Samples were analyzed from -90 °C to 150 °C at 20 °C/min twice to demonstrate hysteresis. All data reported were taken from the second cycle. Glass transition temperatures (T_g)were found using TA Universal Analysis software.

Thermogravimetric Analysis (TGA)

Thermogravimetric analysis (TGA) was performed on a TA Instruments Q50 TGA using a platinum sample pan. The analysis was carried out in the presence of oxygen with breathing air used as the sample gas. Nitrogen was used as the purge gas for the balance. Data were recorded from ambient temperature to 700 °C at a 5 °C/min ramp. Plots of percent weight loss versus temperature were constructed to analyze the data.

Fourier Transformed Infrared Spectroscopy-Attenuated Total Reflectance (FTIR-ATR)

FTIR spectra were recorded on a Thermo Scientific Nicolet 6700 FTIR spectrometer equipped with a Smart Performer ATR attachment with a Germanium crystal at 32 scans. Spectra were recorded from 4000 – 500 cm^{-1} with a resolution of 2 cm^{-1}, and were analyzed using the Nicolet OMNIC software suite.

Raman Spectrometry

Samples were analyzed using either a Nicolet Almega dispersive Raman spectrometer with 10x objective lens and 785 nm or 532 nm excitation laser; or a WiTec Alpha 500 confocal Raman spectrometer with 20x objective and 532 nm laser, at Brookhaven National Laboratory's Center for Functional Nanomaterials; the incident laser spot sizes of these instruments are less than 3 μm.

Gas Chromatography – Mass Spectrometry (GC-MS)

The GC-MS system was an Agilent 7890A gas chromatograph equipped with an Agilent 5975C mass selective detector operating in electron ionization mode and an Agilent 7693A autoinjector. The column utilized was an Agilent HP-5MS (5 % phenyl) methylpolysiloxane film. The carrier gas was helium with a flow rate of 1 mL/min^{-1}. The injection temperature, MS quad temperature, and source temperature were 250 ºC, 150 ºC and 230 ºC, respectively. The detector was set to scan with a mass range of 15 to 250 *m/z*. The temperature program has an initial temperature of 35 ºC for one minute, then 0.5 ºC per minute ramp to 37 ºC followed by a 5 ºC per minute ramp to 80 ºC and then a 20 ºC per minute ramp to 110 ºC with a two minute post run hold at 250 ºC.

X-ray Photoelectron Spectroscopy (XPS)

X-ray photoelectron spectra were obtained using a VG ESCA-3 Mk. II system at ultra-high vacuum (10^{-9} torr). A pass energy of 20eV was used across 50 scans of the sample for each element, in combination with a magnesium K(alpha) anode operating at 120W. Spectra were calibrated using a reference value of 284.0 eV for adventitious carbon.

Scanning Electron Microscopy (SEM)

Micrographs were obtained using an FEI Helios Nanolab dual-beam scanning electron microscope with a secondary electron detector.

Proton (^1H) and Deuterium (^2H) Solid State NMR

Solid State ^1H NMR experiments were done on a Bruker Avance DMX-500 NMR spectrometer using a non-spinning high-power ^1H probe with a horizontal 5 mm solenoidal coil containg the

glass sample tube with film. The ^{1}H NMR spectra and ^{1}H relaxation times were obtained at 500 MHz (11.7 T field).

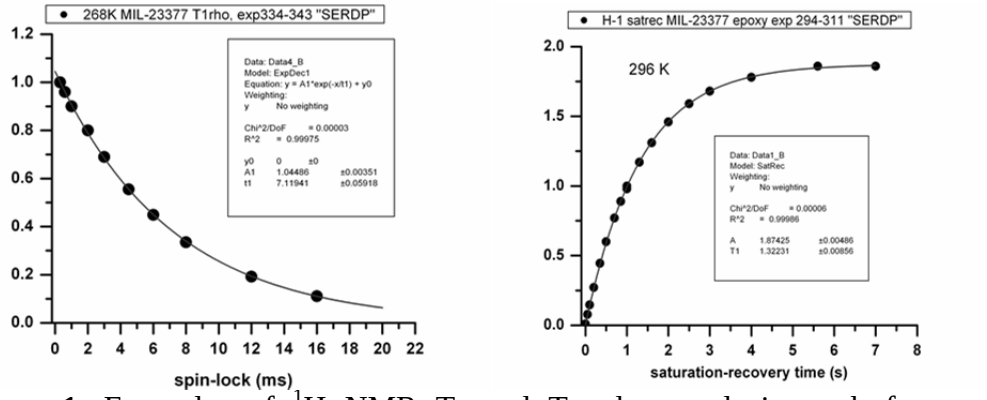

Figure 1. Examples of ^{1}H NMR T_1 and $T_{1\rho}$ data analysis, each for one sample at one temperature.

The ^{1}H spin-lattice relaxation times T_1 were measured using a saturation-recovery pulse sequence with typically a dozen different recovery delays, and fitting the recovery curve of the peak intensity using OriginPro 7.0 to a single-exponential recovery curve with time constant T_1. The intensities of static ^{1}H NMR peaks vs. spin-lock times (typically nine values) in a spin-locking pulse sequence were fit using Origin to a single-exponential decay curve with a decay time constant $T_{1\rho}$. Measurements (Figure 1) were repeated at different temperatures and for different samples.

All of the ^{2}H NMR spectra (nuclear spin I=1) were acquired at 76 MHz on a Varian/Agilent NMR spectrometer at 11.7 T, using a high-power static probe with a 5 mm horizontal solenoidal coil. Spectra of the isotopically-labeled materials were obtained using a quadrupolar-echo pulse sequence ("ssecho1d" provided by Varian) in order to be able to detect the extremely wide (>200 kHz) "powder-pattern" spectra characteristic of ^{2}H in the absence of molecular motions. An error was discovered in the phase-cycling of this manufacturer-supplied program after all experiments were completed. The phases of the last two (out of eight) phase cycles had the phases of the second pulse interchanged from the correct values, which produced two phase cycles where the two pulses were not orthogonal to each other as they should be. However, because the spectra were obtained exactly on-resonance, the net effect of this error was relatively minimal: a reduction of the acquired signal amplitude to 75% of what it should have been, and

some loss in the artifact-removal properties of the phase-cycling. These effects do not affect the data analysis and conclusions presented later.

Results and Discussion

Analysis of neat paint remover

Commercial paint remover (MIL-R-81294) was purchased and analyzed utilizing GC-MS analysis. The presence of methylene chloride (CH_2Cl_2), toluene, ethanol (EtOH), phenol (PhOH) and water were all confirmed; however, the content of each differed as much as 8% from the reported values in Table 1. This was not surprising due to variability in batch manufacture as well as the possibility of chemical reactivity within the can. Additionally, it should be noted that the utility of thickeners and other surfactants could also contribute to the resulting low values for some of the more reactive volatiles. This is expected and a specific rearrangement that may occur is the keto-enol tautomerization shown in Figure 2.

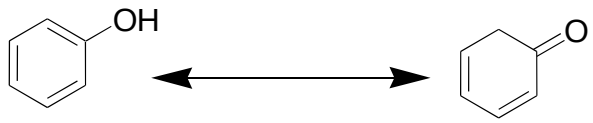

Figure 2. Keto-Enol tautomerization of phenol.

Preparation of clear coatings

The types of resin binders, curing agents, pigments, and additives chosen by a coatings formulator are specifically selected to perform a particular set of functions depending on the performance specifications of the completed coating. The resin/binder and pigment system chosen for a primer is not the best system for a topcoat. The intent in the creation of simplified films was to retain the resin and curing agent ratios while eliminating the pigment portion of the coating to produce clear films of a specified thickness, unsupported or free-standing, for testing purposes.

The removal or change in the amount of one ingredient will affect the performance characteristics of the coating. In the case of pigment removal from a coating, the effect can be catastrophic, much like what would happen if the reinforcements and aggregate were removed from the concrete used in construction. Because they are chemically different, each coating

required major reformulation measures just to form a continuous, uniformly cured film. The various types of coatings and binder types made each of the five coatings a unique challenge.

The biggest challenge was to create 4 mils dry film thickness (DFT) films by applying the clear coatings over a film releasing type substrate utilizing a Byrd applicator. Combining only the resin and curing agent (where applicable) components of the formulas resulted in very thick pasty mixtures that failed to form defect-free films of the uniform thickness required. While thin enough to apply with an adjustable Byrd applicator, films would not release intact from the glass substrate, and "crawled" when applied to plastic coated butcher's paper, waxed paper, and Teflon substrates, forming discontinuous films of varying DFT. Successful release was facilitated using the aircraft release paper, but an even thickness could not be obtained using the drawdown method due to the paper wrinkling under the pressure of the Byrd applicator, and failure of the films to level into a uniform wet film thickness (WFT). In all cases the resin combinations alone were much too viscous to apply with conventional spray equipment. Therefore significant revision/modifications were made to the initial plan.

First, changes were required in the casting of the clear formulations to obtain the required film thickness. Problems were encountered because making a thicker drawdown of the clear material within a WFT range of 10 to 20 mils of a coating that is normally pigmented and designed to be sprayed in much thinner WFT applications ranging from 1 to 2.5 mils creates radically different flow, wetting, curing, and surface tension properties. Attempts at casting the clear formulas were a designed effort to utilize the greater weight of a thick film to overcome surface tension between the substrate and the clear coating, theoretically allowing a continuous, uniformly thick film to form. It was necessary for small amounts of solvent to be added to facilitate better flow and leveling. In the polyurethane formulas, carbon dioxide bubbles evolved during the curing reaction and remained trapped in the film. Further thinning of these formulas, while ridding the film of most entrapped bubbles, didn't prevent bubbles from forming on the surface. The curing of an initially clear polyurethane film would develop into a hazy, bubble entrapped film overnight due to reaction with moisture in the atmosphere. The epoxy clear coatings would only partially cure at the higher casting thicknesses as entrapped solvents prevented complete curing of the film. These films were cloudy looking and remained soft and pliable.

Second, changes were made to the compound formulas by adding the solvents contained in each particular formula in the proportions and thinning ratios specified in order to achieve a workable spray application viscosity. Retaining each specific formula's solvent blend ratio was done to not only reduce formulation variables, but to also minimize the possible impact of varying solvent evaporation rates on curing properties and film formation. Evaporation actions of solvents may cause the formation of Bénard Cells, causing noticeable film imperfections (Figure 3). With thinner films surface tension forces become more crucial.

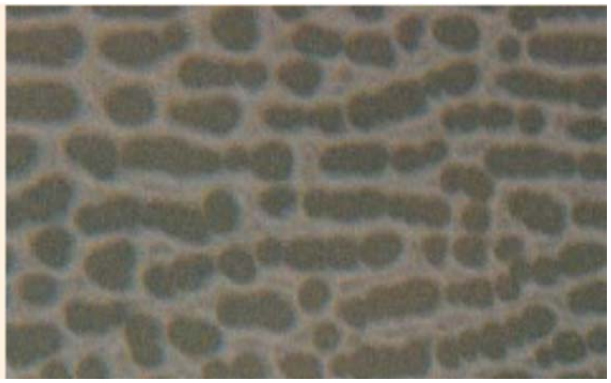

Figure 3. Bénard Cells induced by solvent evaporation due to vortex circulation and change in viscosity. [26]

Third, changes were made to eliminate entrapped carbon dioxide and air by the addition of antifoam agents contained in each formula in the proportions specified. Pigments tend to affect surface tension for the better in flat coatings, almost acting as stabilizers, even aiding in bursting bubbles through surface tension means and physically bursting them, like a pin popping a balloon. When removed, surface tension force effects are often increased, particularly in high gloss coatings and clears resulting in trapped bubbles (Figure 4). Designed to modify a coating's surface tension, including in some cases through the addition of fumed silica to act as tiny glass shards to physically burst the bubble, antifoaming agents utilized in the proper amount will prevent the formation of bubbles on the coating's surface. Too much antifoam additive, or the wrong type, can cause cratering, adhesion problems, and color acceptance problems. Where necessary and when included in the original formulation, anti-foaming agents were retained in the clear formulations and adjusted accordingly.

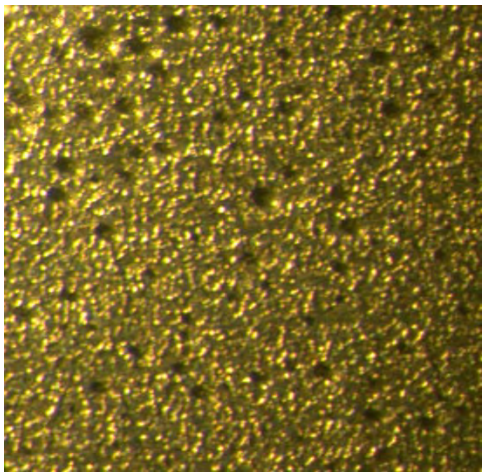

Figure 4. Trapped gas shown in early attempts at clear film application on a chromate aluminum substrate.

Fourth, changes were made to compound formulas to achieve continuous, anomaly-free films of the required thickness requested by utilizing the identical rheology and flow modifiers specified in each formula. Due to the removal of pigments from all formulas, modification of flow characteristics to facilitate the creation of a continuous smooth film of optimal DFT was necessary. Substrate adherence additives and flow modifiers were the key to creating defect-free films (Figure 5).

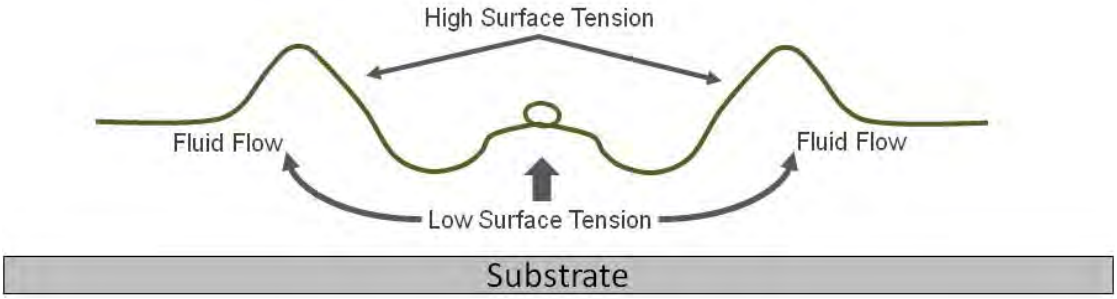

Figure 5. Fisheye and cratering defects due to surface tension differences between the substrate and the coating's top surface.

An example of the effects of a flow modifier on coating film quality is shown in Figure 6. Determination of the right amount of any additive to obtain optimal flow and leveling characteristics is critical.

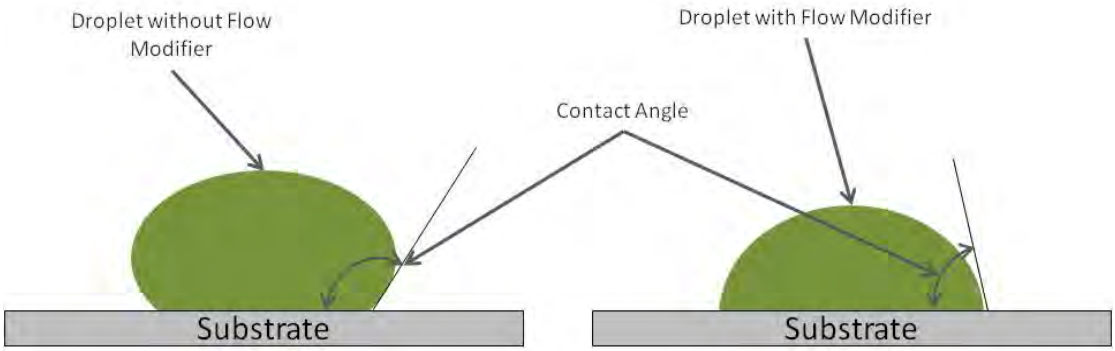

Figure 6. Illustration of how flow modifiers aid in the wetting of the substrate by reducing surface tension.

Fifth, the required clear films were created by spray application rather than by drawdown which was the original plan. Clear films were created after altering the proportions of solvents, adhesion promoters, antifoamers, rheology, and flow modifiers utilized in each clear coating formulation as necessary. Building up the film thickness by spraying multiple coats until achieving the DFT required, though an extremely lengthy process, was the only way to provide the DFT and quality specified. This proved to be the most successful method because it facilitated the application of WFT more in line with the intended design of the original formulation. For the material to cure properly to achieve the required film thicknesses, it was necessary to apply multiple film layers, allowing each to cure before applying another layer. This was crucial to avoid solvent entrapment and the resulting complications.

Comparison of clear, partial formulated and fully formulated coatings

DSC and TGA were also performed on partial formulations of MIL-DTL-53039 and MIL-PRF-85285. These coatings were made by ARL without any flattening agents but with pigments. These coatings were analyzed before and after exposure to a subset of the control solvent mixtures: methylene chloride, a methylene chloride, ethanol and water solution, and a methylene chloride ethanol water and phenol solution. The resulting glass transition temperatures show the same trend seen in the analysis of clear coatings.

Table 11. Glass transition temperatures of clear, partial and fully formulated coatings of MIL-PRF-85285 and MIL-DTL-53039

Glass Transition Temperatures (T_g) in °C						
Solvent Exposure	**Navy/Airforce polyurethane topcoat MIL-PRF-85285**			**Army polyurethane topcoat MIL-DTL-53039**		
	Clear Coatings	Partial Formulation	Full Formulation	Clear Coatings	Partial Formulation	Full Formulation
Control (no exposure)	51	65	0	87	64	60
Methylene Chloride	46	65	15	67	67	76
Methylene Chloride /Ethanol/Water	45	65	26	70	66	81
Methylene Chloride /Ethanol/Water/ Phenol	DECOMP	-19	-38	-11	-25	-8

TGA of the partially formulated coatings response was as expected. They have similar thermal degradation patterns to the clear and fully formulated coatings of the same mil spec. TGA overlays of the three formulations of MIL-DTL-53039 are shown in Figure 7 and those of MIL-PRF-85285 are shown in Figure 8. The final weight of the partial formulated coatings lies between the clear coatings' final weight (approaching zero) and the fully formulated coatings' final weight. The fully formulated coatings have a large amount of inorganic material mostly pigments and flatteners where the partial formulated coatings have only flatteners. The inorganic material remains on the TGA pan as a final weight since this material is not altered at temperatures used during the run. The clear coatings would be predicted to have a final weight approaching zero since they contain no pigments or flatteners.

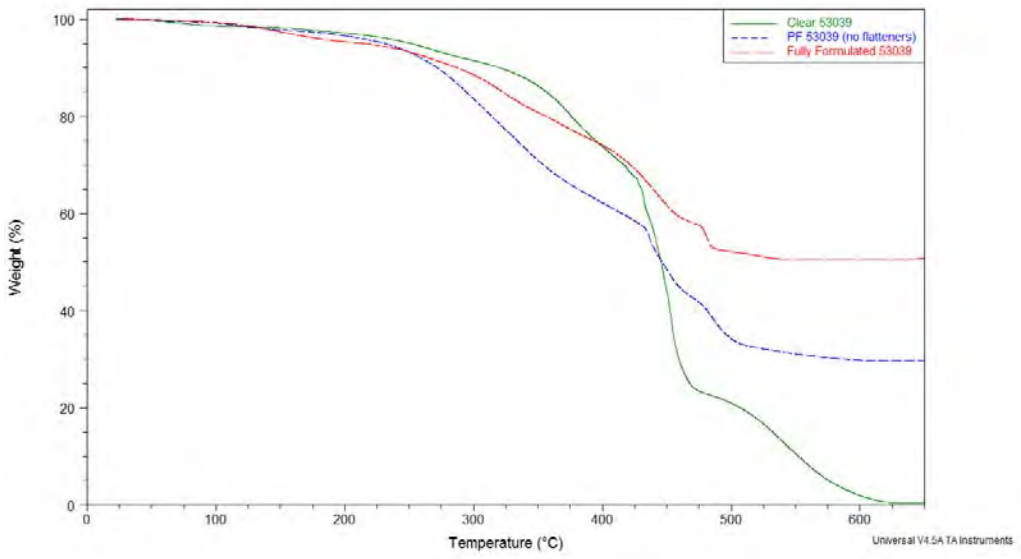

Figure 7. TGA overlay of the three formulations of control (unexposed) coatings of CARC polyurethane topcoat (MIL-DTL-53039)

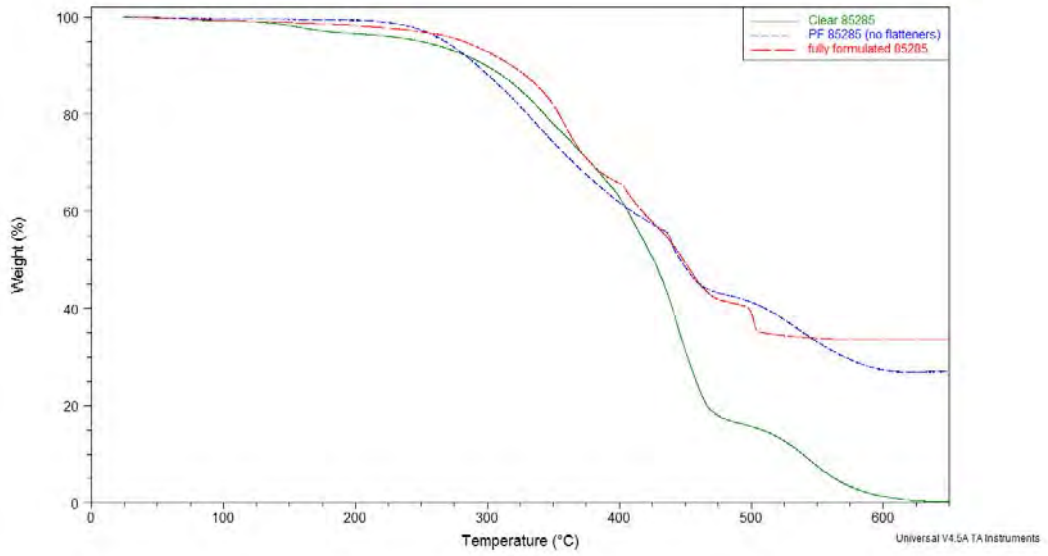

Figure 8. TGA overlay of the three formulations of control (unexposed) coatings of NAVY topcoat (MIL- PRF-85285)

TGA overlays of the partial formulation MIL-DTL-53039 exposed to different solvent mixtures are seen in Figure 9. Overlays for the partial formulation of MIL-PRF-85285 exposed to the same solvent mixtures are seen in Figure 10. The results of thermal analysis of clear coatings compared to fully and partially formulated coatings before and after exposure to control solvent mixtures clearly illustrate the use of the simplified coating system. Although the presence of pigments, filler and flatteners have an effect on the basic value of the glass transition

temperature, the trends and changing of the T_g upon exposure is independent of the presence of this inorganic particles. The weight of incombustibles remaining at the end of the TGA run is, understandably, altered by the presence of pigments, fillers and flatteners but again the changes after exposure do not appear affected.

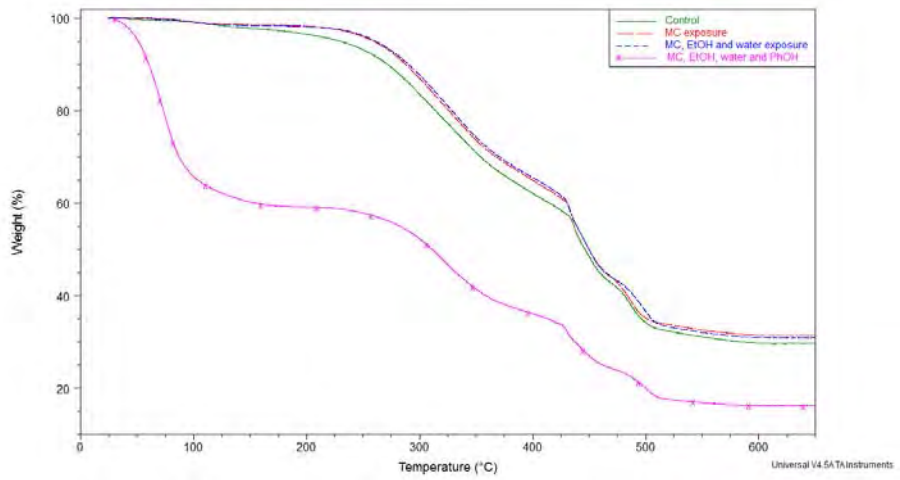

Figure 9. TGA overlay of Partially Formulated CARC polyurethane topcoat (MIL-DTL-53039) exposed to different solvent mixtures

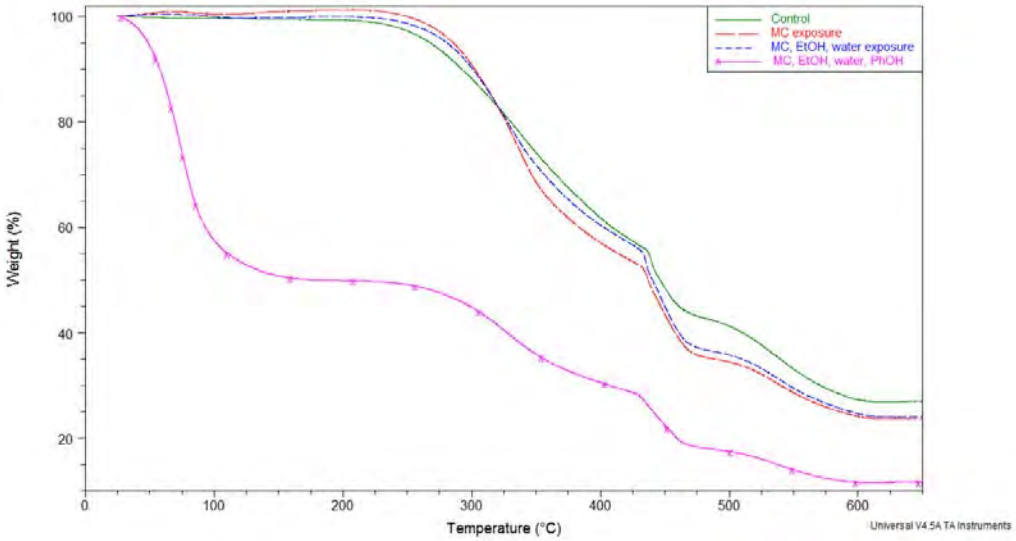

Figure 10. TGA overlay of partially formulations of NAVY polyurethane topcoat (MIL- PRF-85285) exposed to different solvent mixtures

Initial characterization of samples

Samples of fully formulated chemical agent resistant coating (CARC) paint (MIL-DTL-53039) as well as NAVY/Air Force topcoat (MIL- PRF-85285) were prepared on release paper and characterized for baseline measurements using Fourier transformed infrared spectroscopy - attenuated total reflectance (FTIR-ATR), thermogravimetric analysis (TGA) and differential scanning calorimetry (DSC). The purpose of this preliminary study was to determine that the method and instrumental technique was not only compatible with the individual instrument, but also to determine that the sample thickness was sufficient to perform under the specified method once the control formulation coatings become available.

Upon receiving the clear control films, characterization by FTIR-ATR ensured the correct functionalities were present as well as provided a snapshot as to the degree of curing by examining free unreacted functional groups. After observing satisfactory results, TGA analysis was performed to ensure the absence of nontraditional species such as inorganic additives. All coatings demonstrated less than 1 wt. % incombustible material in a breathing air atmosphere, which was acceptable for subsequent analyses.

Thermal analysis of clear coatings

In an attempt to find evidence of chemical and physical changes, DSC was employed on each of the clear coatings upon exposure to controlled combinations of the depaint ingredients as seen in Table 12. This was followed by analysis of the exposed clear coating using TGA. The control solutions of phenol (PhOH) with methylene chloride and separately with ethanol (EtOH) were tested for the effect on the coatings after observation of the significant change to the coatings exposed to the mixture containing phenol. DSC was performed on all exposed coatings while TGA was only performed on coatings exposed to solvent for two hours. The solutions used for thermal studies are shown in Table 1.

Table 12. Reported glass transition values of clear coatings from DSC.

		MIL-DTL-53039	MIL-PRF-85285	MIL-PRF-85582	MIL-PRF-23377	MIL-PRF-53022
Control		87	51	62	40	67
2 hour exposure	CH_2Cl_2	67	46	74	49	81
	CH_2Cl_2 & EtOH	67	44	76	48	85
	CH_2Cl_2, EtOH & Water	70	45	77	48	75
	CH_2Cl_2, EtOH, Water & PhOH	-11	decomp	decomp	17	61
	CH_2Cl_2 & PhOH	-4	-30	-18	-22	73
	EtOH & PhOH	-9	-25	-33	-19	41
Two day exposure	CH_2Cl_2	72	44	70	51	70
	CH_2Cl_2 & EtOH	65	41	76	49	69
	CH_2Cl_2, EtOH & Water	70	43	82	51	75
	CH_2Cl_2, EtOH, Water & PhOH	-4	decomp	decomp	-5	62

For coating MIL-DTL-53039, the one-component CARC polyurethane, it was also noted that exposure to ethanol and phenol caused the coating to separate into two layers with different physical properties, although each layer had similar T_g values. Exposure to methylene chloride and phenol results in the onset of delamination; however, no other solvent(s) causes such separation, making it unreasonable to assume that the separation results from film preparation.

The TGA for MIL-DTL-53039 both before and after exposure can be seen in Figure 11. The TGA of the coatings exposed to mixtures without phenol are all similar to that of methylene chloride alone. All of these mimic the shape of the TGA control coating except a larger weight loss by 150 °C. The TGA of the coatings exposed to phenol containing mixtures show immediate weight loss and a different graph shape including a more severe (~50%) weight loss by 200 °C. Measurement of the TGA of the phenol and ethanol exposed coating was preempted by the coating's separation into two layers.

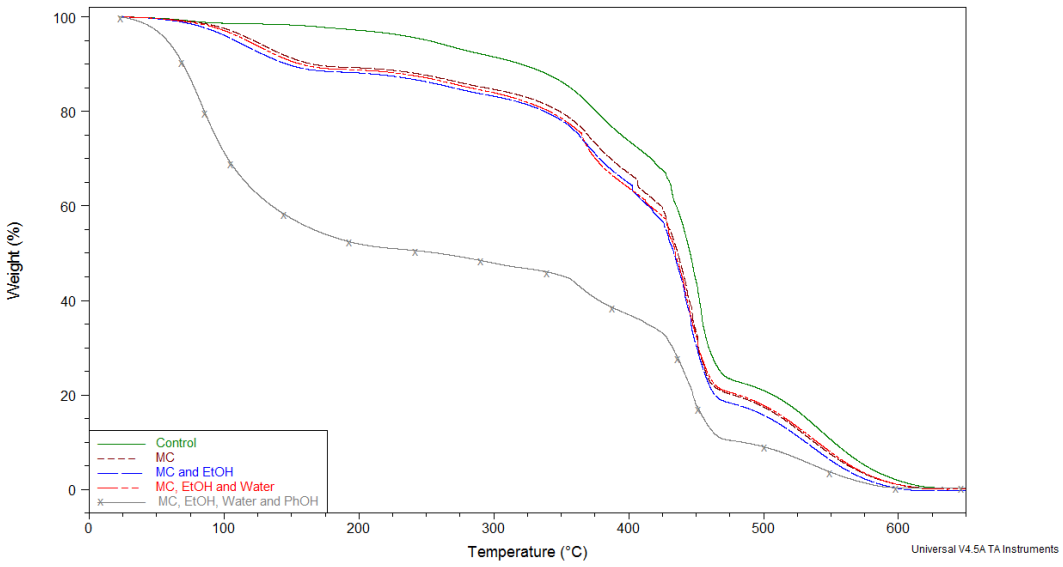

Figure 11. TGA overlay for clear CARC polyurethane topcoat (MIL-DTL-53039)

For coating MIL-PRF-85285, the two-component polyurethane NAVY topcoat, the sample of this coating that was exposed to methylene chloride, ethanol, water and phenol however, decomposed into small pieces preventing DSC or TGA analyses. The TGA results for this coating (MIL-PRF-85285) can be seen in Figure 12. They follow the same patterns as the TGAs of MIL-DTL-53039.

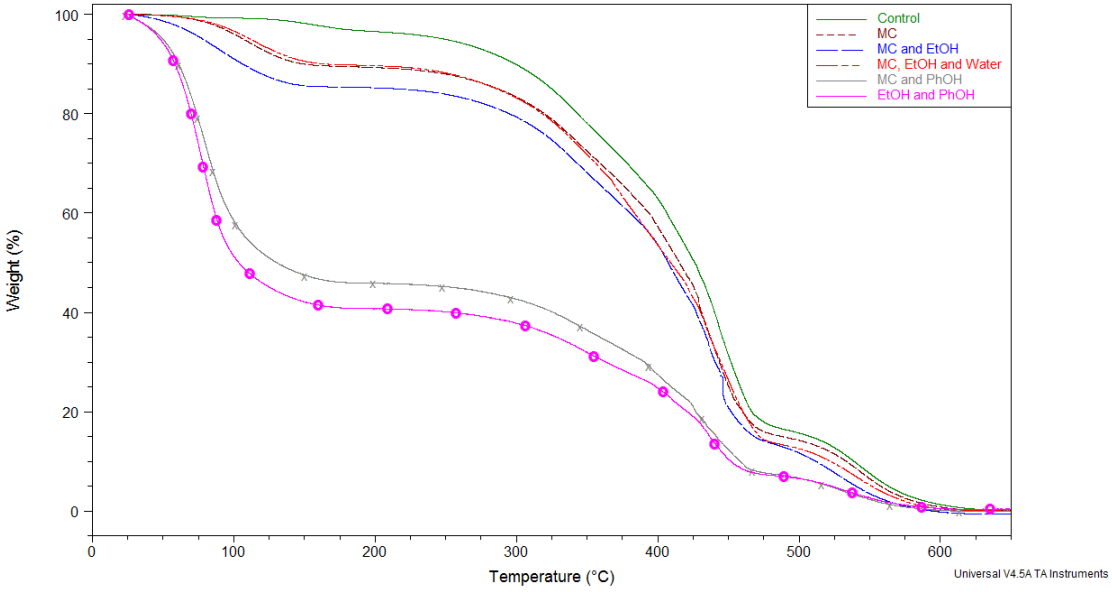

Figure 12. TGA overlay for clear NAVY polyurethane topcoat (MIL-PRF-85285).

For coating MIL-PRF-85582, the water-borne epoxy primer, the sample of this coating that was exposed to methylene chloride, ethanol, water and phenol decomposed into small pieces, like MIL-PRF-85285, preventing DSC and TGA analysis. The TGA of the MIL-PRF-85582 coatings can be seen in Figure 13.

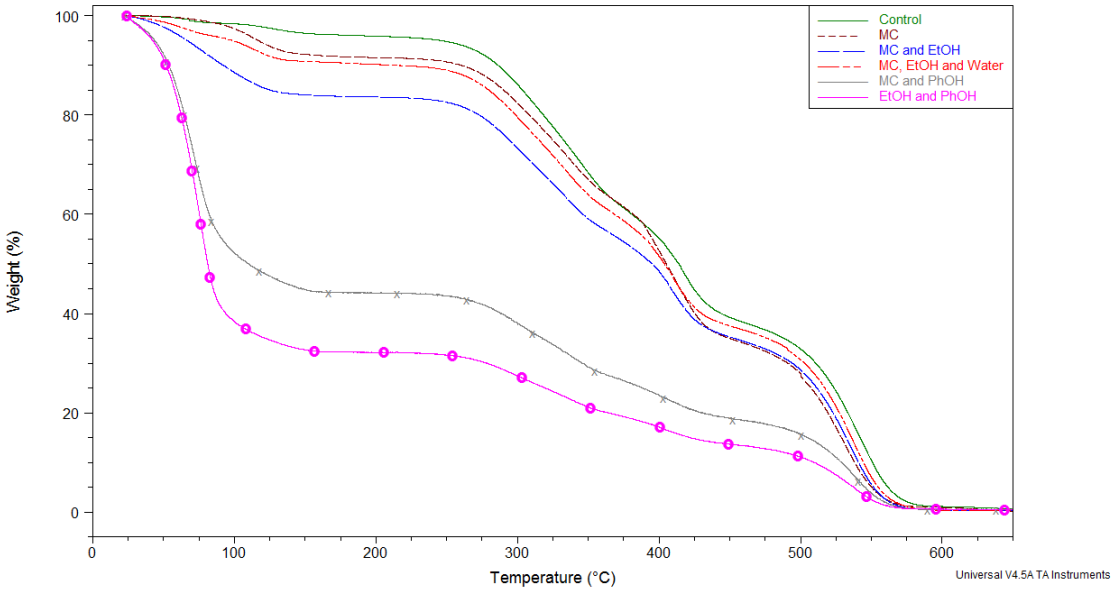

Figure 13. TGA overlay for clear Waterborne Epoxy Primer (MIL-PRF-85582).

For MIL-PRF-23377, the two-component solvent-borne epoxy primer, it appears that the analysis process is most likely resulting in additional crosslinking of the already highly crosslinked system. The TGA of the MIL- PRF-23377 coatings can be seen in Figure 14.

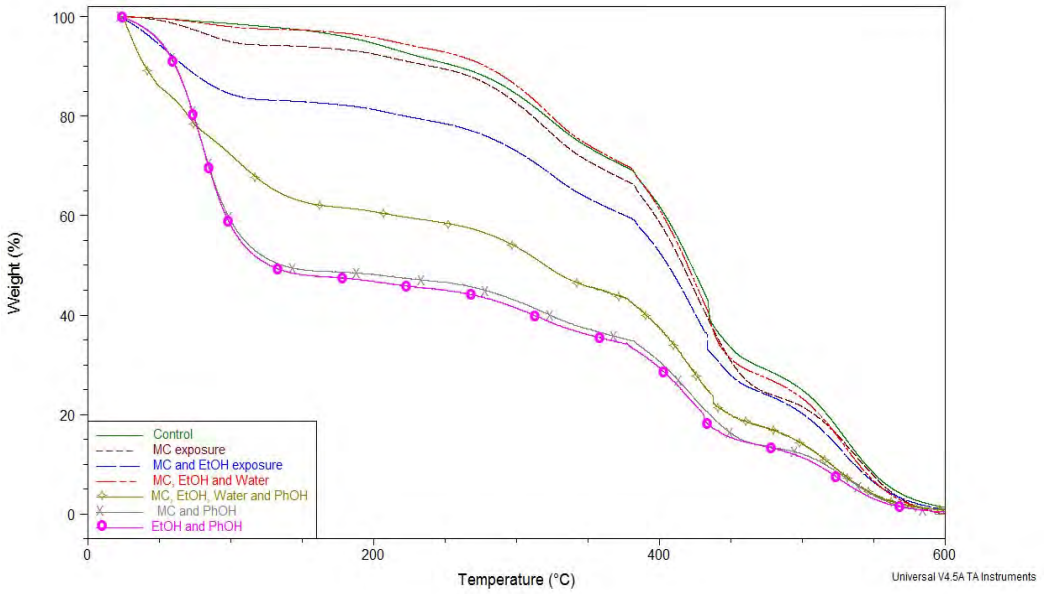

Figure 14. TGA overlay for clear Polyamide Epoxy Primer (MIL- PRF-23377)

For coating MIL- PRF-53022, the epoxy primer, the degradation profile is unchanged by exposure. Exposure to the solvent mixtures has a limited effect, primarily increasing the weight loss at low temperatures. The exposure to the methylene chloride, ethanol, water and phenol solution does not dramatically change the TGA profile as seen in other coatings. The TGA for the MIL- PRF-53022 coatings can be seen in Figure 15.

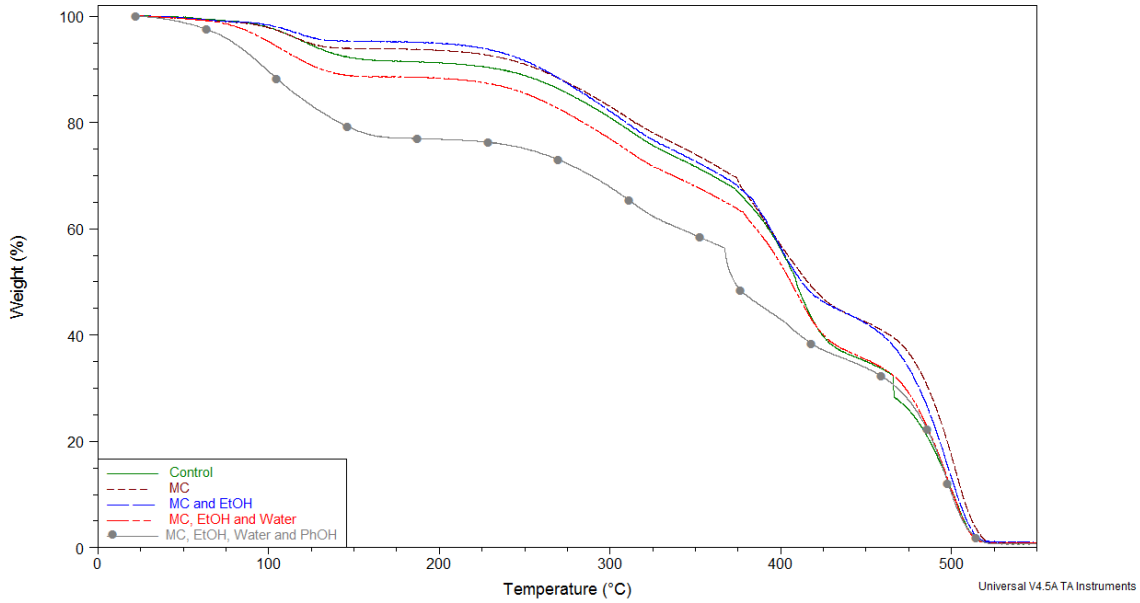

Figure 15. TGA overlay for clear Epoxy Primer (MIL- PRF-53022).

Color Change and Headspace Analysis

It was noted, some weeks after testing the samples, that coatings which had been exposed to a solvent mixture containing phenol exhibited a color change. The original coating samples are clear or slightly opaque. MIL-DTL-53039 and MIL-PRF-85285 turn a pink color after exposure to phenol while MIL-PRF-85582 and MIL-PRF-23377 turn an orange color. Figure 16 shows an example of the color change. The pink coating on the left is MIL-DTL-53039 (the CARC polyurethane topcoat) after exposure to methylene chloride, ethanol, water and phenol. The orange coating on the right in Figure 16 is MIL-PRF-23377 (the polyamide epoxy primer) after exposure to methylene chloride and phenol.

Figure 16. Examples of clear coating's color change after exposure to phenol solution (clear MIL-DTL-53039 on left, MIL- PRF-23377 on right)

A weight loss is seen in the TGA at temperatures lower than 100 °C for coatings exposed to solvent mixtures containing methylene chloride, ethanol, water and phenol in any combination. This weight loss was not seen in the unexposed coatings. A method was devised to determine if the exposure solvents were trapped in the clear coatings at room temperature. Small portions of exposed coatings were heated in small air-tight vials and then the head space vapors were injected into the GC/MS. The resulting chromatograms show that methylene chloride, ethanol and phenol are being trapped in the clear coatings at room temperature and released upon heating. Methylene chloride and ethanol are seen weeks after drying while phenol is seen months after drying.

Thermal analysis of fully formulated coatings

Fully formulated coatings were also examined by thermal analysis. The first difference noted between the fully formulated and clear coatings was that the DSC of unexposed coating (control) gave a lower glass transition temperature (T_g) for the fully formulated coatings than for the clear coatings in all formulations except MIL- PRF-23377. Two of the coatings, MIL- PRF-53022 and MIL- PRF-85285, have T_g below room temperature and so are somewhat rubbery/flexible at room temperature.

Fully formulated coatings were exposed for two hours to five separate solvent mixtures previously used with the clear coatings: methylene chloride alone, a methylene chloride and ethanol solution, a methylene chloride, ethanol and water solution, a methylene chloride, ethanol, water and phenol solution, a methylene chloride and phenol solution and an ethanol and phenol solution. It was observed that the fully formulated coatings react somewhat differently than the clear coatings upon solvent exposure, as can be seen in the table of T_g's below (Table 13). The exposure of the first three solvent mixtures did not significantly change the T_g of the clear coatings. However these exposures caused large increases in the T_g for the fully formulated coatings. The exposure to the phenol containing solutions caused a severe decrease in most of the fully formulated coatings. The methylene chloride, ethanol, water and phenol solution gives the greatest decrease in T_g from the control for all the fully formulated coatings. The other two phenol containing solutions decreased the T_g to a lesser extent except in MIL- PRF-53022. For all the fully formulated coatings the ethanol and phenol solution has a less pronounced effect than the methylene chloride and phenol solution.

Table 13. Glass transition temperatures for clear and fully formulated coatings after a two hour exposure to control solvent solutions

	MIL-PRF-23377 epoxy primer		MIL-PRF-85582 epoxy primer		MIL-DTL-53039 Polyurethane topcoat		MIL-PRF-85285 Polyurethane topcoat		MIL-PRF-53022 epoxy primer	
	clear	fully formulated	clear	fully formulated	clear	fully formulated	clear	fully formulated	clear	fully formulated
Control	40	65	62	50	87	60	51	0	67	10
MC	49	91	74	102	67	76	46	15	81	83
MC/EtOH	48	93	76	100	67	76	44	22	85	81
MC/EtOH/ Water	48	103	77	103	70	81	45	26	75	93
MC/EtOH/ Water/PhOH	17	-2	DECOMP	-12	-11	-8	DECOMP	-38	61	-20
EtOH/PhOH	-19	56	-33	4	-9	-13	-25	-45	41	38
MC/PhOH	-22	36	-18	21	-4	-2	-30	-54	73	15

TGA of the fully formulated coatings were done before and after exposure to the same control solvent solutions used to test the clear coatings.

TGA for fully formulated coatings exposed to methylene chloride, methylene chloride/ethanol and methylene chloride/ethanol/water were performed. The TGA of these exposed coatings differ from those of the clear coatings, but in general do not differ from the control. In all the fully formulated coatings the exposed samples show less weight loss than the controls, which is opposite of what was seen with the clear coatings. MIL- PRF-23377 (see Figure 20) shows little difference after exposure compared to control. The shape of the TGA curve after exposure looks very similar in shape to the control for MIL- PRF-23377, MIL- PRF-85285 (see Figure 18) and MIL- PRF-53022 (see Figure 21). The TGA curves for MIL- PRF-85582 (see Figure 17) vary

somewhat depending upon exposure and MIL-DTL-53039 (see Figure 19) exposed coatings TGAs look similar in shape to each other just different from the control.

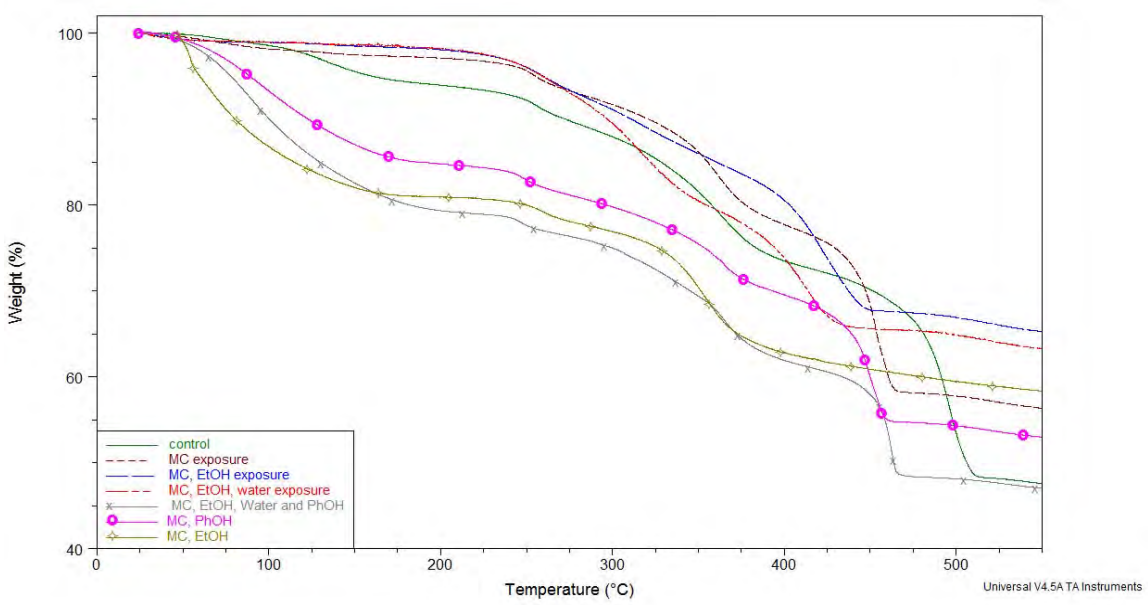

Figure 17. TGA overlay of fully formulated waterborne epoxy primer (MIL- PRF-85582)

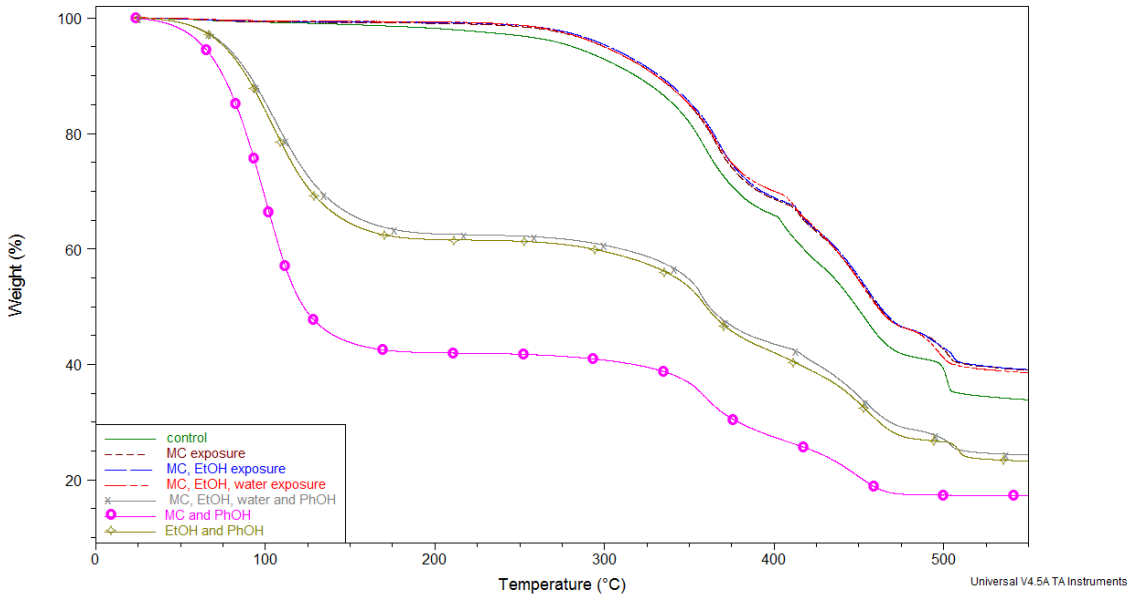

Figure 18. TGA overlay of fully formulated NAVY polyurethane topcoat (MIL- PRF-85285)

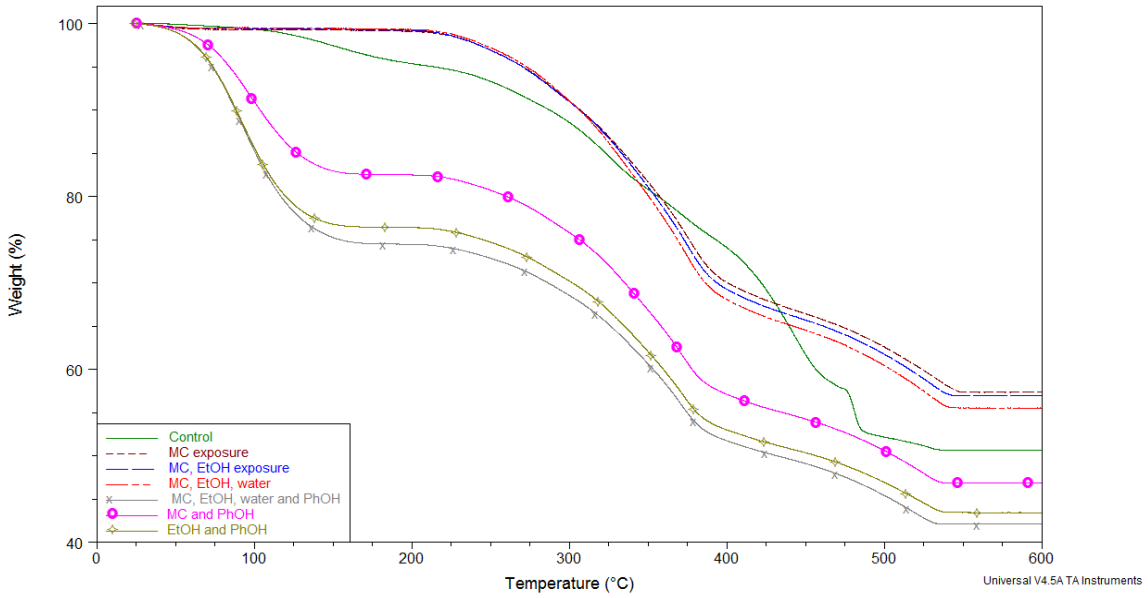

Figure 19. TGA overlay of fully formulated CARC polyurethane topcoat (MIL-DTL-53039)

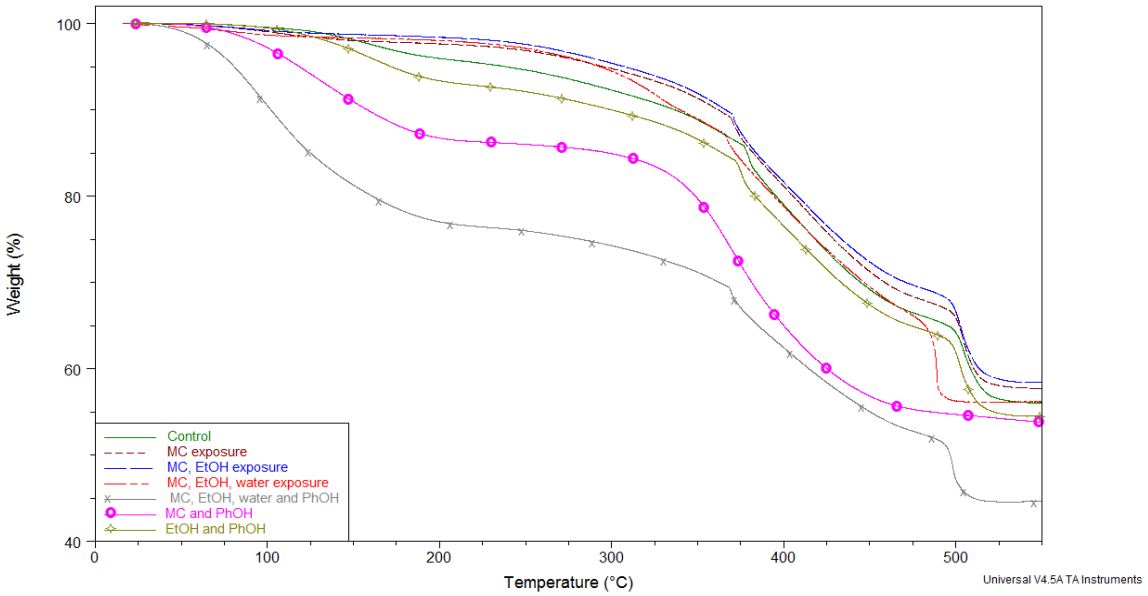

Figure 20. TGA overlay of fully formulated polyamide epoxy primer (MIL- PRF-23377)

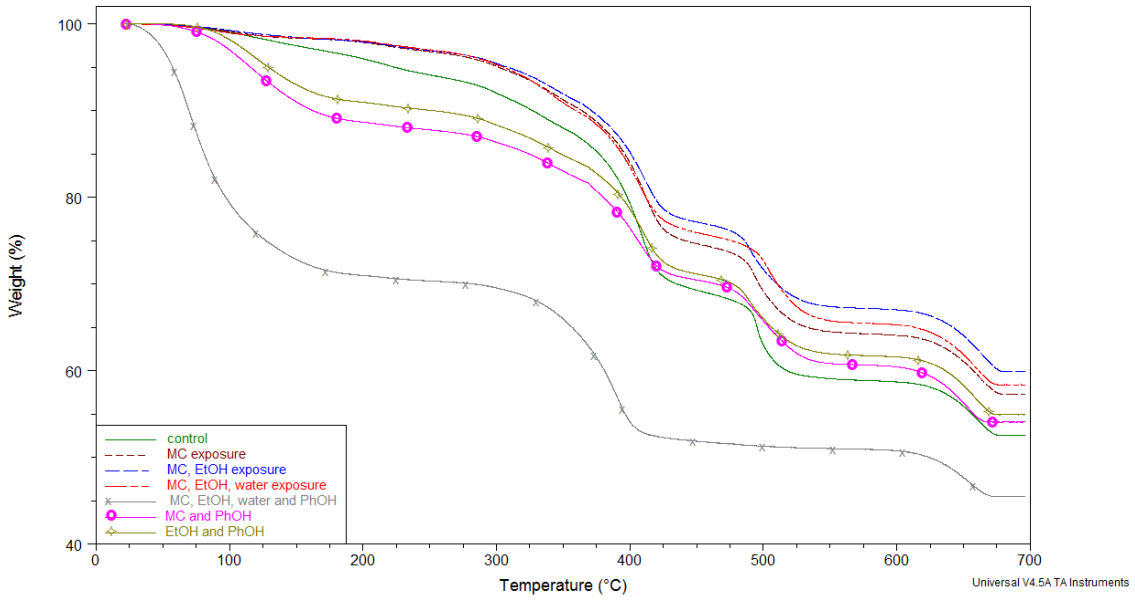

Figure 21. TGA overlay of fully formulated epoxy primer (MIL- PRF-53022)

Exposure to the phenol containing solutions (methylene chloride/ethanol/water/phenol, methylene chloride/phenol and ethanol/phenol) produce similar TGA results in the fully formulated coatings as in the clear coatings, mainly a substantial weight drop at the low temperatures while maintaining the same degradation profile as the control coating. For all the coatings except MIL- PRF-85285, the four component control solvent solution exposure caused the greatest weight drop. In MIL- PRF-85285 the methylene chloride/phenol solution created the largest weight decrease.

Vibrational Spectroscopy

In order to create a mechanistic model the chemical changes induced by solvents drawn from the paint stripper were evaluated using Raman and FTIR spectroscopic analyses. FTIR and Raman spectra have been obtained for each sample before and after exposure to the selected solvent mixtures.

The clear formulation of the two polyurethane topcoats, MIL- PRF-85285 and MIL-DTL-53039, were subjected to equivalent exposure conditions and vibrational spectra were taken of both. While exposed to methylene chloride, both coatings exhibit an increase in flexibility and are swelled. The Raman shows significant broadening of the C=O vibration while the coating is solvated with methylene chloride, as seen in Figure 22, which shows the Raman spectra of the

two component topcoat MIL-PRF-85285 before and during exposure to methylene chloride. This broadening suggests that the solvent is affecting inter-chain dilation at the hydrogen-bonding links C=O…H-N. The carbonyl vibration peak broadening is more pronounced in the two component topcoat MIL-PRF-85285 than in the waterborne topcoat MIL- DTL-53039. After being removed from the solvent, the effect on the C=O peak disappears within 15 minutes, which is confirmed by a swelling collapse after solvent outgassing. Figure 23 shows the Raman spectra of the waterborne topcoat MIL- DTL-53039 immediately following overnight exposure to methylene chloride. Three spectra are shown with increasing time from the coating's removal from methylene chloride. Physically the sample returns to approximately its original stiffness after removal from methylene chloride. Methylene chloride may not cause any permanent chemical changes to the polymer. However this induced dilation explains the ability of methylene chloride to facilitate the penetration into the coating of other components in the solvent mixture.

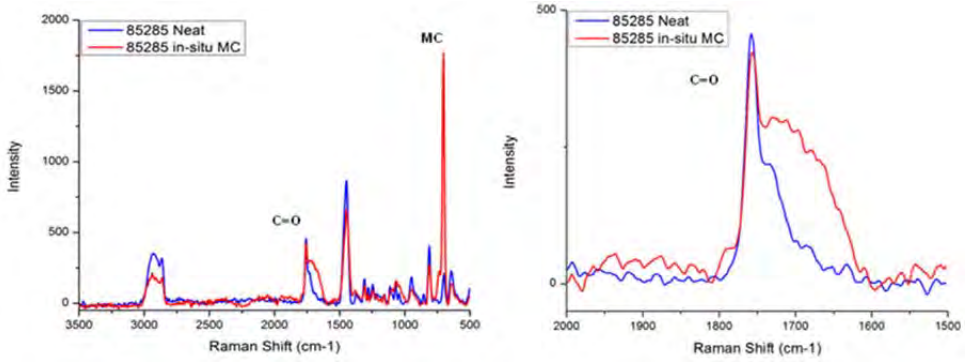

Figure 22. Raman spectra of NAVY polyurethane topcoat (MIL-PRF-85285) alone and saturated with methylene chloride, zoom of C=O region

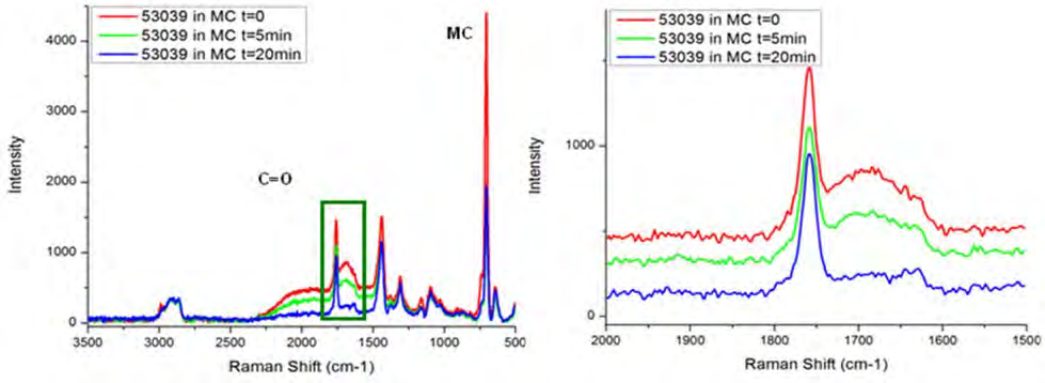

Figure 23. Raman spectra of CARC polyurethane topcoat (MIL- DTL-53039) exposed to methylene chloride, zoom of C=O region

Analysis of the FTIR spectra of the clear coatings before and after exposure to control solvent solutions of methylene chloride and methylene chloride/ethanol depicts no considerable changes, as can be seen in Figure 24. In the spectrum of the methylene chloride/ethanol exposed coating there is a minor peak decrease at 1683 cm^{-1}, corresponding to the infrared-active C=O vibration. The carbonyl bond dilation is unlikely to be present. It is reasonable that the solvents have evaporated from the top 2µm of the film and the dilation or other changes in the coating cannot be detected using FTIR.

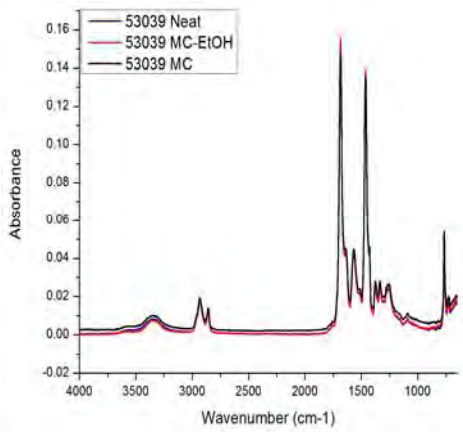

Figure 24. FTIR-ATR spectra of CARC polyurethane topcoat (MIL- DTL-53039) before and after exposure to methylene chloride and methylene chloride/ethanol solution

Figure 25 shows the Raman spectra of MIL- DTL-53039 before and after exposure to methylene chloride and ethanol (82:8) as well as a magnified view of the carbonyl region of the spectrum at 1747 cm^{-1}. Several extra peaks are visible; these correspond to components of the solvents applied. Here, methylene chloride and ethanol are detected readily within the sample, even after extended periods of drying. Considering the comparatively short exposure time of the analyzed sample (15 minutes) as compared to drying time (two hours), the significant presence of solvent components within the coating must be indicative of solvent entrapment by the matrix. The spectra show a minor height decrease and shift in the carbonyl (C=O) peak at 1747 cm^{-1}, as a result of exposure to solvents containing methylene chloride; there is a broadening and shift of approximately 2 cm^{-1}. This confirms the dilation of the hydrogen bonds between the polyurethane chains (C=O---H-N) by methylene chloride, supporting the notion that methylene chloride acts to facilitate penetration into the coating of larger solvent molecules.

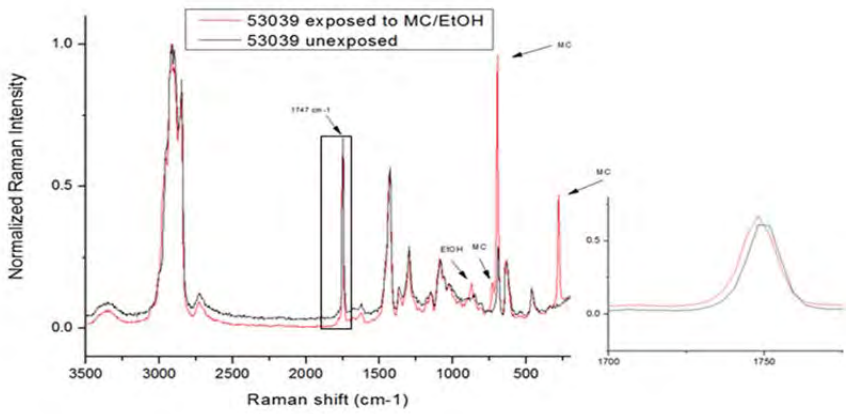

Figure 25. Raman spectra of MIL-DTL-53039 before and after exposure to methylene chloride and ethanol including an expansion to resolve the carbonyl peak.

The waterborne polyurethane sample (clear MIL-DTL-53039) showed visible changes to relative opacity of the sample after exposure to a methylene chloride, ethanol and water mixture; localized clear regions were observed. FTIR analysis of these clear regions has shown interesting chemical changes. With exposure to a solvent mixture of methylene chloride, ethanol and water, FTIR shows a decrease in the carbonyl peak and evidence of new ether and alcohol groups. There is a dramatic decrease in the strength of the C=O vibration at 1683 cm^{-1}, with a corresponding formation of peaks at 1186, 1151, 1112, and 1061 cm^{-1}, representing a series of stretches occurring in a C-O-C system. These can be seen in Figure 26. A similar effect is seen in the solvent mixture containing methylene chloride, ethanol, water and phenol; however, spectral overlap of phenol with many possible affected bonds has interfered with any mechanistic analysis. The presence of phenol within the sample after a very long drying period indicates that phenol is bound within the sample somehow, via either steric hindrance or chemical bonding to the surrounding resin.

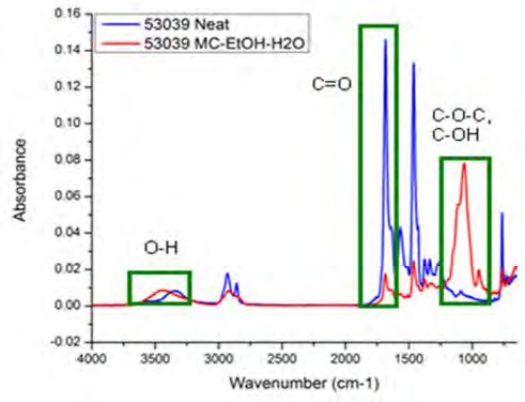

Figure 26. FTIR of MIL- DTL-53039 before and after exposure to MC/EtOH/Water solution

X-ray photoelectron spectroscopy (XPS) was used to investigate the effects of solvent exposure by a mixture of methylene chloride, ethanol and water on the clear coating MIL-DTL-53039. XPS analysis highlighted distinct changes in the carbon (1s), nitrogen (1s) and oxygen (1s) spectra of the coating following exposure that match well with previous results. In Carbon 1s (Figure 27), the peak indicative of C=O is greatly diminished, which is also seen by ATR-FTIR analysis. The lack of broadening in the main Carbon 1s feature shows that any newly-formed bonds are of similar binding energy to the pre-existing carbon-nitrogen and carbon-oxygen bonds. In FTIR, this is seen by the formation of C-O-C and C-OH.

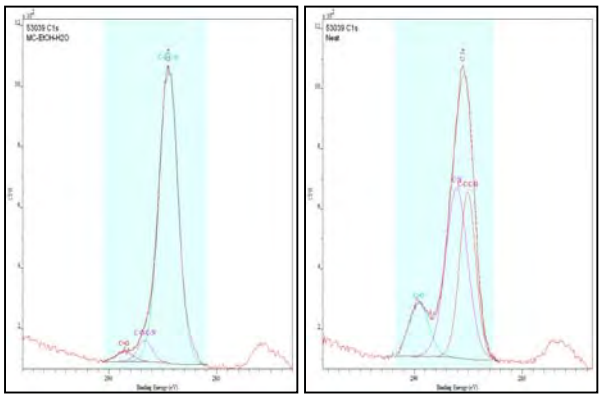

Figure 27. XPS of carbon (1s) in clear CARC polyurethane topcoat (MIL-DTL-53039) before and after exposure to methylene chloride/ethanol/water solution

The oxygen 1s spectrum further corroborates these changes, see Figure 28. Broadening of the main feature indicates the presence of the O-C and OH peaks seen by FTIR.

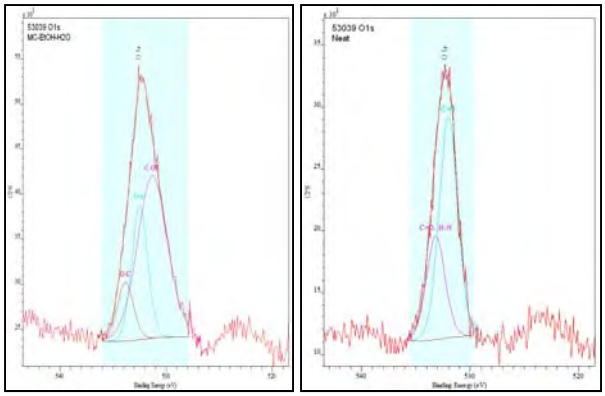

Figure 28. XPS of Oxygen (1s) in clear CARC polyurethane topcoat (MIL-DTL-53039) before and after exposure to methylene chloride/ethanol/water solution

The nitrogen (1s) spectrum is severely diminished by solvent exposure (Figure 29). This indicates that the solvent either induces a conformational change that depletes nitrogen from the surface, or the reactions that result in the formation of the new bonding states seen above also result in the elimination of nitrogen from the polymer. It should be noted that these changes are not visible using Raman spectroscopy. We speculate that it is because the changes are all occurring at the surface, and the Raman instrument used has a very high sampling depth in clear materials, while ATR-FTIR and XPS are highly surface-sensitive (2µm and 10nm, respectively).

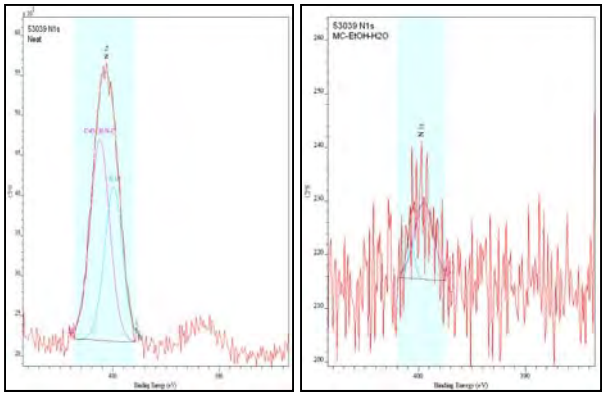

Figure 29. XPS of Nitrogen (1s) in clear CARC polyurethane topcoat (MIL-DTL-53039) before and after exposure to methylene chloride/ethanol/water solution

We speculate that the evolution of C-O-C and C-OH at the surface of the coating is caused by a hydrolysis reaction, given that these peaks only form in the presence of water. The presence of Methocel as a stabilizer could also account for this surface chemistry, so further steps were taken to verify its absence. Samples were washed extensively in methylene chloride/ethanol after exposure in order to remove any trace of surface contamination. After this cleaning, the visible

changes to the coating remained, indicating that a chemical reaction had occurred. SEM analysis of clear coating MIL-PRF-85285 after exposure to methylene chloride, and to methylene chloride/ethanol/water shows no damage after exposure to the former, and visible surface degradation after exposure to the latter (Figure 30).

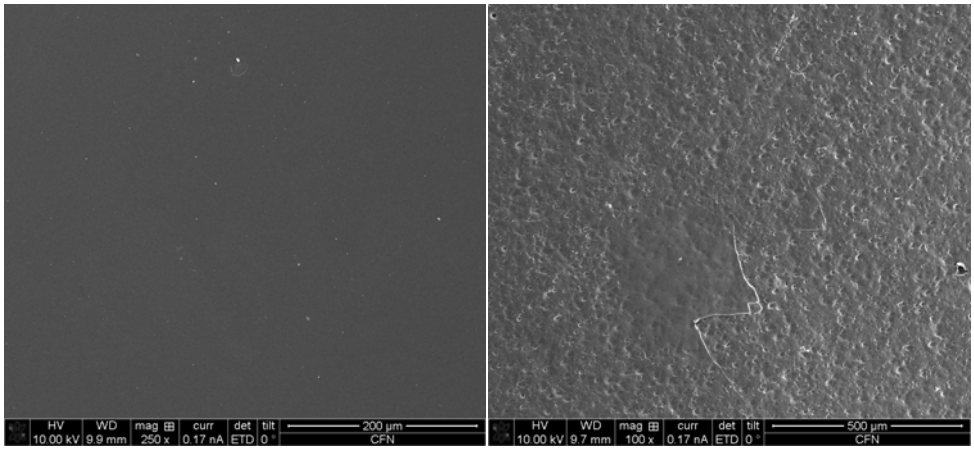

Figure 30. Electron micrographs of coating MIL-PRF-85285 exposed to (left) methylene chloride and (right) methylene chloride/ethanol/water, demonstrating significant surface changes as a result of exposure.

Exposure to liquid phenol also results in significant swelling and softening of the coating which does not diminish even after extensive drying. The sample acquires a slight color indicative of the presence of impure solid phenol. There is no broadening of C=O in the FTIR-ATR after methlyene chloride/ethanol exposure as seen after methylene chloride exposure. The spectrum of phenol dominates the FTIR spectrum, obscuring the peaks of the polymer, making the evaluation of chemical changes extremely difficult. This is consistent with the previously noted color change and GCMS headspace analysis.

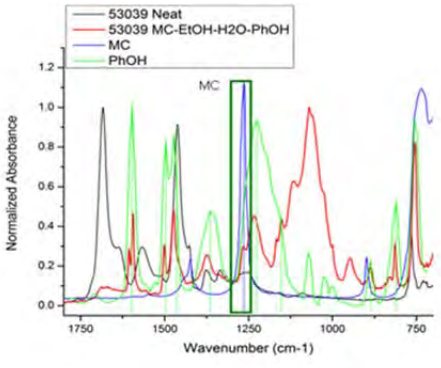

Figure 31. FTIR spectra demonstrating solvent persistence after drying in CARC polyurethane topcoat (MIL-PRF-53039)

Figure 32 depicts the Raman spectroscopic result of the exposure of clearcoat CARC polyurethane topcoat (MIL-DTL-53039) to a mixture of the solvents methylene chloride, ethanol, water and phenol. Here, phenol is the dominant solvent component visible in the spectra; methylene chloride is not visible. The most significant effect of this solvent is the reduction in intensity of the peaks corresponding to C=O (1750 cm^{-1}) and CH_2/CH_3 stretching (around 3000 cm^{-1}). This indicates a reduction in presence of these components but precise quantitative conclusions cannot be drawn from these results. There is also a small increase in the region of 1060 cm^{-1}, corresponding to C-O-C ether stretching.

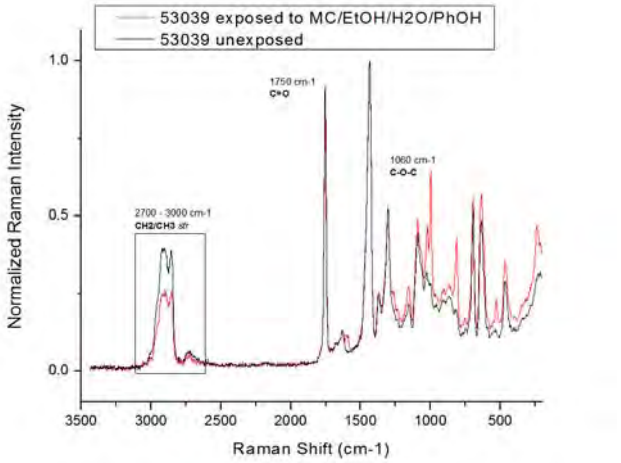

Figure 32. Raman spectra of CARC polyurethane topcoat (MIL-DTL-53039) before and after exposure to a mixture of methylene chloride, ethanol, water and phenol

The infrared spectrum of the same exposure, shown in Figure 33, provides even more interesting results. The peak representing C=O (around 1683 cm^{-1}) diminishes drastically, and a series of peaks indicative of ether C-O-C stretches (1167, 1152, 1117, 1069, 1025 and 1000 cm^{-1}) appear with moderate intensity. There is an obvious chemical change occurring.

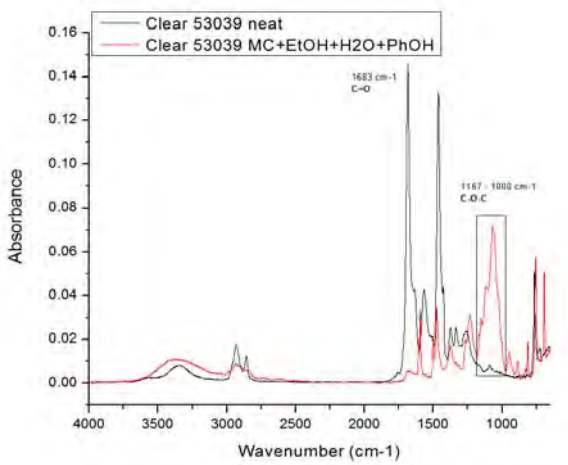

Figure 33. FTIR spectra of CARC polyurethane topcoat (MIL-DTL-53039) before and after exposure to a mixture of methylene chloride, ethanol, water and phenol.

In light of the apparent effects of phenol, a separate experiment was performed exposing the waterborne polyurethane MIL-DTL-53039 coating to liquid phenol (89 % PhOH, 11 % H_2O). Physically, the effects of this exposure are dramatic - the coating quickly dissolved into a shapeless mass after exposure. The Raman spectrum before and after this exposure is seen in Figure 34. Even after several days of outgassing, significant quantities of phenol remain within the sample. There is significant reduction in peak intensity and area in the region around 3000 cm^{-1}, corresponding to CH_3 and CH_2 stretching modes. Reduction is also seen at 1750 cm^{-1}, corresponding to C=O stretching. An increase is seen in the vicinity of expected ether stretches (1060 cm^{-1}) as well. Specific identification of the peaks is complicated by the presence of phenol as its vibrations overlap many of the areas likely regions for peak formation.

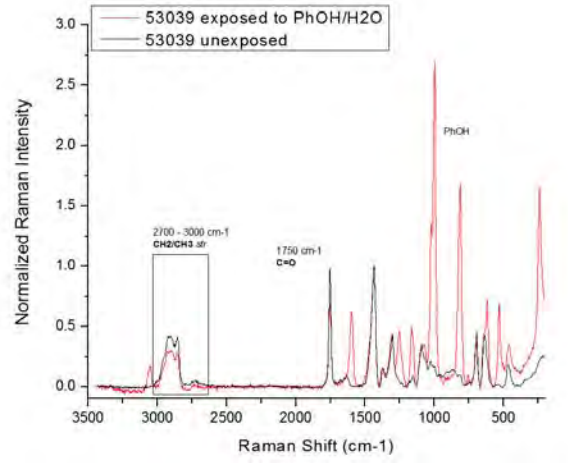

Figure 34. Raman spectra of CARC polyurethane topcoat (MIL-DTL-53039) before and after exposure to phenol and water

Solid State NMR Analysis

In order to obtain molecular level information about the effects of solvents upon clear coatings using a very different spectroscopic approach, solid-state proton (^{1}H) and deuterium (^{2}H) NMR were employed. The ^{1}H NMR results provided information about the segmental dynamics of the polymer chains in the topcoat and epoxy as a function of temperature and solvent exposure. The ^{2}H NMR results provide molecular-level information about the solvent molecules themselves, by relying upon isotopic-labeling of the methylene chloride or phenol components.

^{1}H Solid-state NMR of Topcoat (Clear coat) and MC Exposed Sample

In the ^{1}H NMR spectra the full-linewidth at half-height (HHLW) is decreased by segmental dynamics of polymer chain on time scales < 20 μs. The spin-lattice relaxation time T_1 is governed by fast dynamics on a ns time scale (Figure 35). The spin-lattice relaxation time in the rotating frame ($T_{1\rho}$) is affected predominantly by slow motions (having a ~ 15 μs time scale), of the type that may permit solvent diffusion into polymer (Figure 35). By performing these measurements as a function of temperature, dynamics induced by a rise in temperature can be compared with dynamics induced by solvent swelling.

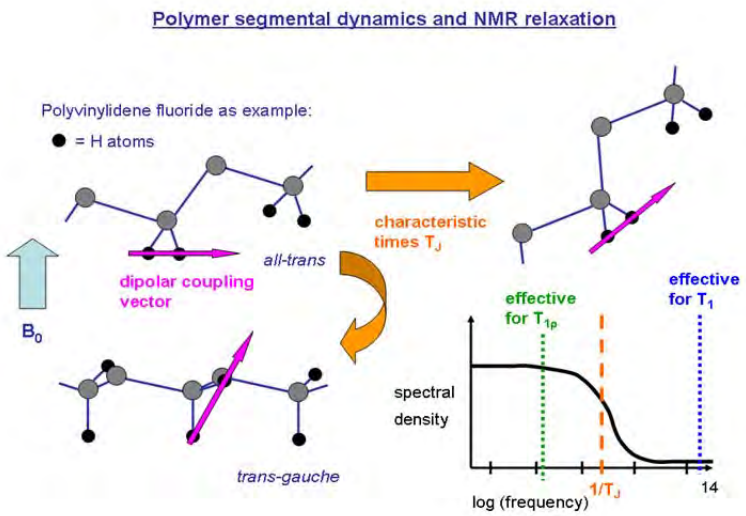

Figure 35. Schematic example of polymer segmental dynamics affecting ^{1}H NMR relaxation through modulation of proton-proton dipolar coupling.

Figure 35 shows a schematic example of how polymer segmental dynamics (local conformational change in bottom molecule, longer-range reorientation of chain in top right molecule) modify the orientation of the internuclear proton-proton dipolar coupling vector with respect to the external magnetic field B_0. The resultant modulation of the dipolar coupling is responsible for NMR relaxation. The characteristic jump times involved, T_J, represent a correlation time for an assumed random process that can be related to a Lorentzian spectral density as shown in the log plot, with a cut-off frequency of $1/T_J$. For a dynamic process with the cut-off depicted, increasing temperature would raise the cut-off frequency while keeping the integrated spectral density constant, resulting in less-effective $T_{1\rho}$ relaxation (longer $T_{1\rho}$) and more-effective T_1 relaxation (shorter T_1).

The polyurethane topcoat clear film sample (MIL-DTL-53039) CARC was selected as the first sample to examine using the strategy described in the materials and methods section. The ^1H NMR results from the unexposed sample were compared with those from the same sample exposed to methylene chloride for 5 minutes. Figure 36 shows T_1 vs. temperature for the film before and after exposure to methylene chloride, as well as the T_1 for the neat solvent alone.

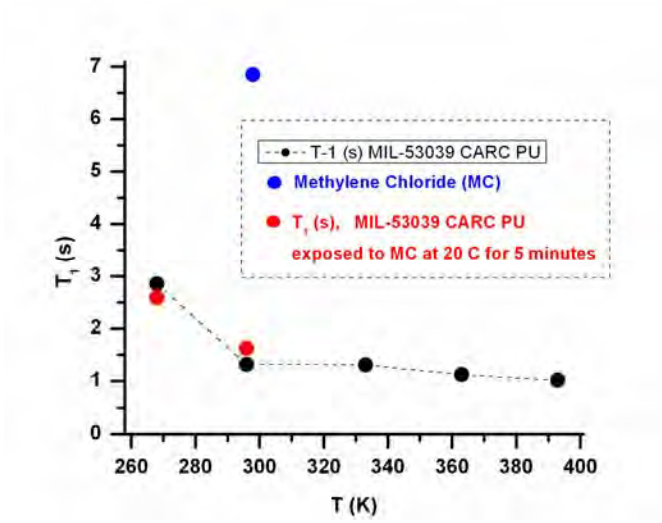

Figure 36. Proton NMR T_1 vs. temperature for MIL-DTL-53039 before and after 5-minute exposure to methylene chloride at 20 °C. Also shown is the T_1 of neat methylene chloride.

Several conclusions can be drawn from these data. The T_1 of neat methylene chloride is long because it is an isotropic liquid with a short (ns) rotational correlation time, whereas the T_1 of the unexposed polymer film is significantly shorter and typical of non-rigid polymers. The near-equality of the two T_1 values of the polyurethane sample exposed to methylene chloride to those

in the starting polyurethane film at the same temperature indicates that methylene chloride is in intimate atomic-scale contact with the polymer, since the proton NMR signal from the methylene chloride component contributes to the overall spectrum of the exposed sample. This intimate contact results in the methylene chloride having significant proton-proton dipolar coupling to the polyurethane polymer, which equalizes T_1 values by the process known as spin-diffusion. There is no evidence whatsoever for free methylene chloride in liquid-like pools of any size, which would yield a sharper proton NMR peak having a longer T_1.

In addition to these T_1 experiments on this same polyurethane film before and after exposure to methylene chloride, the $T_{1\rho}$ experiments as summarized in Figure 37 were conducted. The steep drop in $T_{1\rho}$ values for the unexposed film above the maximum around 330 K can be interpreted as due to the activation of relatively slow motions on a approximately 15 μs time scale (the optimum for $T_{1\rho}$ relaxation at the rf field strength used, corresponding to a T_J of 15 μs in Figure 37).

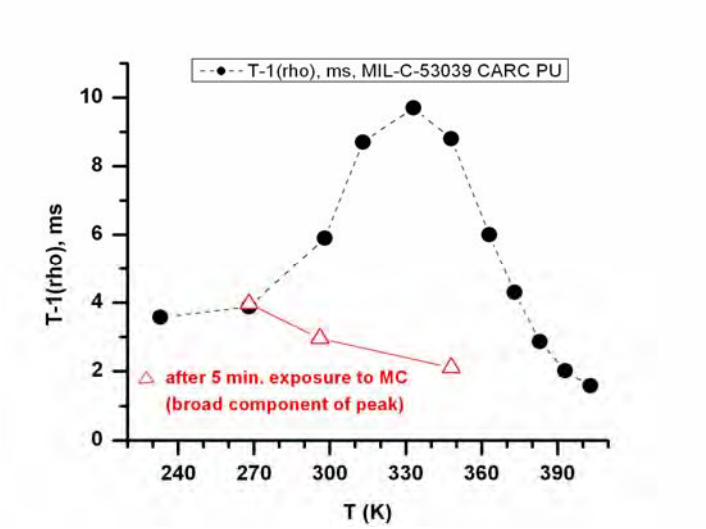

Figure 37. Proton NMR $T_{1\rho}$ vs. temperature for MIL-DTL-53039 film before and after 5-minute exposure to methylene chloride at 20 °C.

The proton NMR spectra of the CARC polyurethane topcoat (MIL-DTL-53039) clearcoat film are shown in Figure 38. The spectrum obtained at 296 K (23 °C) is greatly broadened by homonuclear dipolar interactions (ca. 50 kHz half-height linewidth), as expected for a crosslinked polymer with only limited segmental dynamics (the T_g measured above was 87 °C). Heating the sample to near the T_g (363 K, or 90 °C) results in a substantial reduction in the

linewidth due to greatly increased segmental dynamics that partially average out the dipolar interactions.

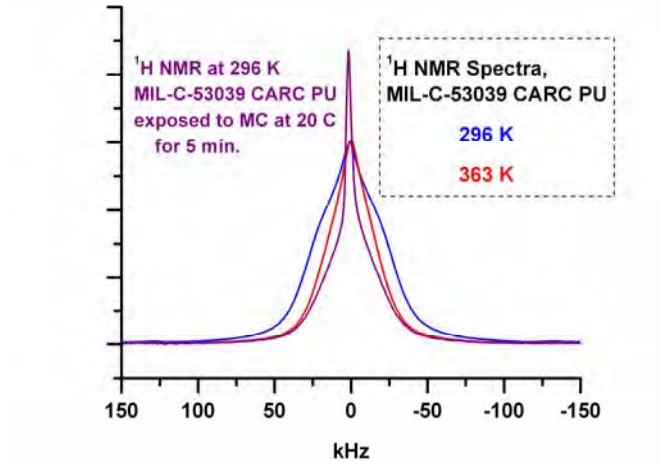

Figure 38. Wideline proton NMR spectra of MIL-DTL-53039 at two different temperatures, and after exposure to methylene chloride.

Similarly, exposure to methylene chloride for 5 minutes at 20 °C results in a spectrum at 296 K that is greatly narrowed by an increase in the segmental dynamics, similar to the effects of increasing temperature alone. (The T_g reported above of this sample after 2 hours exposure to methylene chloride was 67 °C.) The lineshape also has the appearance of a sharper and a broader component, the former of which is still broader than would be the case for purely liquid-like pools of methylene chloride. It is reasonable to attribute the sharper component to methylene chloride that is so strongly dipolar-coupled to nearby polymer protons that it shares the same T_1 relaxation time (Figure 38).

^{2}H Solid-state NMR of Topcoat (Clear coat) Exposed to CD_2Cl_2 (d_2-MC)

The deuterium NMR spectra of the CARC polyurethane topcoat (MIL-DTL-53039) clearcoat film after 10 minute exposure to deuterated methylene chloride are shown in Figure 39. The room temperature (24° C) CD_2Cl_2 narrow linewidth indicates rapid rotational motion, but not rapid enough to be liquid solvent. The spectrum reveals that all of the CD_2Cl_2 molecules are undergoing rotational motion sufficiently rapid enough (less than 10 μs) to average out the rigid-lattice nuclear quadrupole coupling constant, NQCC (see the later section on ^{2}H NMR of d_5-

phenol for a reference to simulations of the effect of motions on the spectra). The 1.4 kHz HHLW (half height linewidth) is still broader than what is expected for the neat solvent.

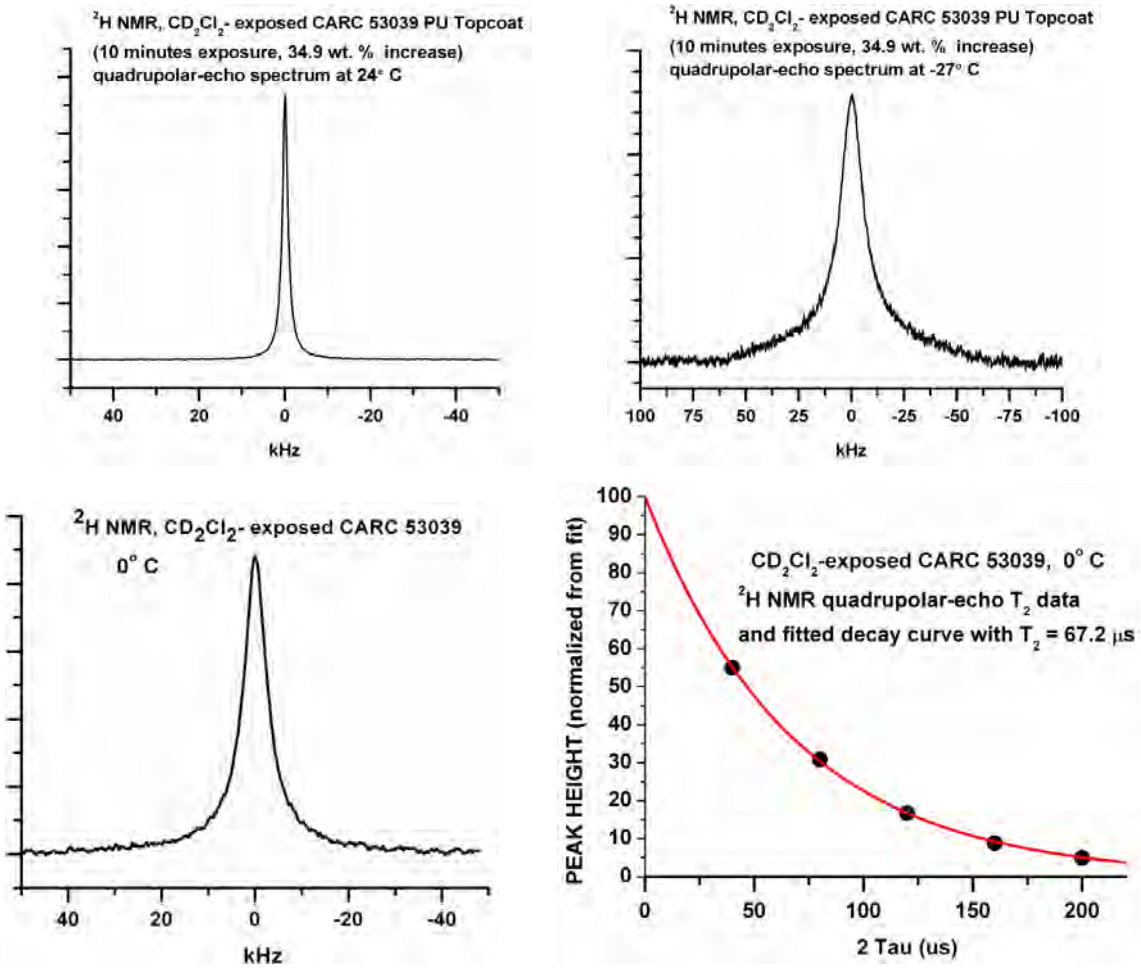

Figure 39. Deuterium quadrupole-echo NMR spectra of CD_2Cl_2 exposed CARC polyurethane topcoat (MIL-DTL-53039) at three different temperatures as indicated, and measurement of T_2 transverse relaxation time at 0º C

Cooling the sample to 0º C resulted in a broader spectrum that could be fitted very well to a Lorentzian lineshape with a HHLW = 6.3 kHz, broader than the linewidth at 24º C. The T_2 value measured by varying the delay tau in the quadrupolar-echo sequence and fitting to a single-exponential decay was 67.2 μs, as shown in Figure 39. This value corresponds to a homogeneous linewidth of 4.74 kHz. The difference of 1.6 kHz from the (larger) measured linewidth seems too large to be accounted for by broadening due to magnetic susceptibility or field inhomogeneities. It may be due to a distribution of small residual quadrupolar splittings that somehow do not result in a deviation from a Lorentzian lineshape. The measured T_2 is many orders of magnitude shorter than that expected for pure CD_2Cl_2 (hundreds of milliseconds or

greater). The relevant equation for the full HHLW of the Lorentzian in the motionally-narrowed regime is $\Delta\omega_0^2\ \tau_c / \pi$ (in Hz), where s $\Delta\omega_0^2$ is the second moment (in angular frequency units) characterizing the rigid solid linewidth and τ_c the rotational correlation time.[27] The latter depends upon the molecule or particle size and the viscosity of the medium, and is typically 10^{-11} s for a small molecule such as CD_2Cl_2 in a low-viscosity solvent. Thus, the measured T_2 and corresponding broad homogeneous linewidth indicate that the CD_2Cl_2 molecule in the CARC MIL-DTL-53039 coating at 0º C has a rotational correlation time of the order of three orders of magnitude *greater* than its value in neat CD_2Cl_2. Although one cannot assign a meaningful viscosity to the surrounding polymer matrix, it is clear that the rotational tumbling of the CD_2Cl_2 molecule is being restricted, quite plausibly by some sort of electric dipole-electectric dipole interaction with polar groups on the polymer. The fact that the spectrum is not that of an immobilized solvent molecule indicates that the interaction energy is relatively weak compared to the thermal energy kT.

The spectrum at reduced temperature (-27 ºC) of deuterated methylene chloride after swelling the CARC polyurethane topcoat (MIL-DTL-53039) is significantly broader than the spectra obtained at either 24º C or 0º C (note the different frequency scale). The HHLW is 14.1 kHz, but also apparent is an even broader peak at the base. This indicates a further degree of restriction to the rotational motion of the solvent molecules upon further cooling, and possibly the existence of two different environments.

^{1}H Solid-state NMR of Primer (Clearcoat) and Phenol/Ethanol Exposed Sample

An NMR strategy similar to that employed with the topcoat above was used to investigate the epoxy (polyamide) primer MIL-PRF-23377 clearcoat film, whose T_g of 40 °C reported above is much lower than that of the polyurethane topcoat (87 °C). The ^{1}H NMR half-height linewidths as a function of temperature are shown in Figure 40. The solvent proton NMR signals did not appear as sharp peaks that would be the case for liquid-like pools, but instead as broadened indistinct features in the spectrum. Because they represent a minor proton-containing component in the exposed sample, their contribution to the linewidth can be neglected to a first approximation. It is interesting to note that although the polyurethane and the epoxy polymers do not have the same chemical structure, the effective number density of their hydrogen atoms may be comparable, which in turn would yield comparable ^{1}H NMR linewidths for both in the

rigid lattice limit (at low temperatures). Consequently, the approximately 50 kHz HHLW of the polyurethane film at 296 K is consistent with the fact that for the epoxy this broad linewidth is achieved only at approximately 230 K (-43 °C), which in both cases is about 80 °C below the respective T_g values.

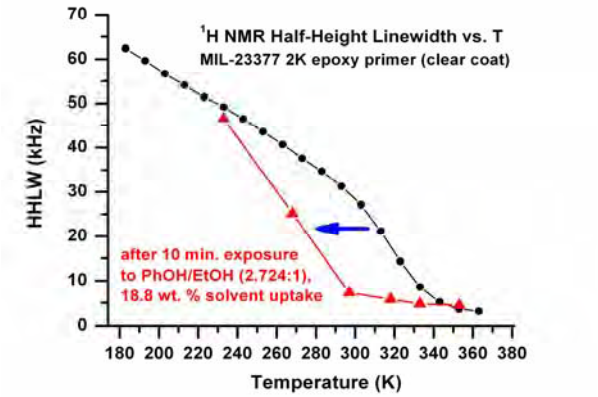

Figure 40. Proton NMR half-height linewidths vs. temperature for MIL-PRF-23377 before and after exposure to phenol/ethanol.

The effect of a 10-minute exposure to a phenol/ethanol mixture (2.724:1), which resulted in a 18.8 wt. % solvent uptake, upon the linewidth vs. temperature is also shown in Figure 40. The solvent exposure has markedly shifted the temperature at which a marked decrease in linewidth occurs, by roughly 40 °C. A somewhat larger decrease in the T_g, by 59 °C, was observed by DSC after a two hour exposure to the same solvent mixture. It is clear that this solvent combination alone can significantly affect segmental dynamics of the epoxy clearcoat film even after a short 10-minute exposure.

The ^{1}H $T_{1\rho}$ relaxation time vs. temperature for this same epoxy clearcoat film before and after a 10 minute exposure at 20 °C to the same phenol and ethanol mixture (2.724:1) is shown in Figure 41.

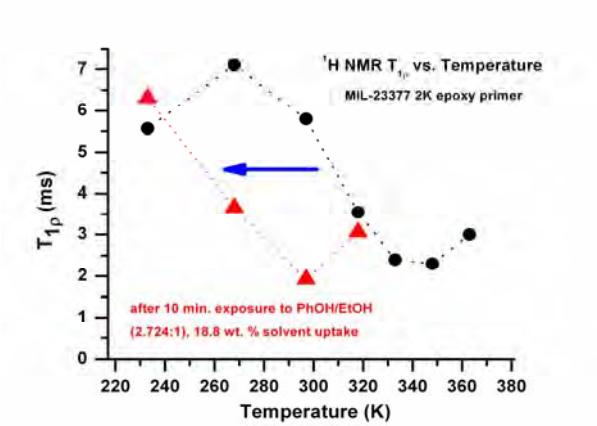

Figure 41. Proton NMR $T_{1\rho}$ relaxation times for MIL-PRF-23377 vs. temperature, before and after exposure to phenol/ethanol for 10 minutes at 20 °C.

Several points are worth noting. For the unexposed film, a clear minimum in $T_{1\rho}$ is observed at approximately 340 K (67 °C). As discussed above for the $T_{1\rho}$ results on the polyurethane film, this implies that slow segmental dynamics on a (T_J) time scale of 15 μs have their maximum spectral density at this temperature. In other words, segmental dynamics occurring at a rate of 70 kHz are activated and maximized when the temperature is raised to 340 K., which is some 27 °C above the measured T_g. The relationship deduced between the segmental dynamics associated with the polymer glass transition and the measured $T_{1\rho}$ values is supported by the (slightly extrapolated) $T_{1\rho}$ minimum for the polyurethane topcoat film at approximately 410 K in Figure 37, which would correspond to 37 °C above its T_g.

The effect of exposure to the phenol and ethanol solution upon the temperature dependence of $T_{1\rho}$ shown in Figure 41 is to shift the curve roughly 50 °C towards lower temperature. This results from the increased polymer segmental dynamics after solvent exposure, and is consistent with the similar shift of approximately 40 °C noted above for the linewidths.

^{2}H Solid-state NMR of Solid d_5-Phenol and of Primer (Clear coat) Samples Exposed to d_5-Phenol/Ethanol Mixtures

The ^{2}H quadrupolar-echo NMR spectrum of solid *d_5*-phenol at 24º C, below its melting point of 41º C, is shown in Figure 42. Solid *d_5*-phenol, where the hydrogens on the phenyl ring have been replaced by deuterium, exhibits a very wide (129.4 kHz splitting of the "horns") spectrum characteristic of a 172.5 kHz nuclear quadrupole coupling constant (NQCC) and zero asymmetry parameter η. This arises from a rigid molecule that does not undergo the "flips" of the phenyl

ring observed in other situations; the rigidity is reflected in the long recycle delay of 60 s needed to avoid saturating the signal. The sharp central peak seen in Figure 42 (HHLW = 130 Hz), which was observed to have a T_1 relaxation time substantially shorter than that of the broad quadrupole-split pattern, may arise from a small amount of highly mobile phenol molecules. A similar sharp peak was observed in previously reported ^{2}H spectra at 300 K and 295 K, but not 250 K.[28] Curiously, the "horns" of our spectrum are much sharper than those observed in the previous study, which in addition to a nearly-identical splitting of the horns (131 kHz) also reported a sole single rather sharp peak at 310 K, which is 4º below the melting point. It remains unknown whether this is due to an error in measurement of the sample temperature, sample impurities and consequent melting point depression, an intensification of the central sharp peak relative to a broader peak that because of a shortened T_2 becomes unobservable in the quadrupolar echo, or complete nearly isotropic mobility of all phenol molecules in the lattice.

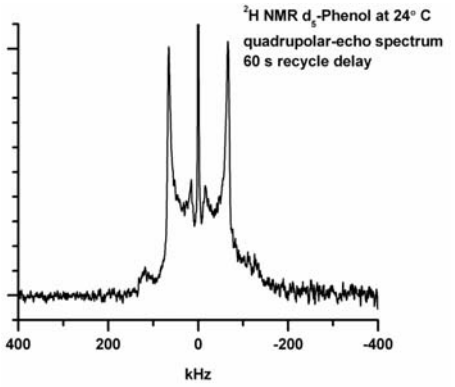

Figure 42. ^{2}H quadrupolar-echo NMR spectrum of solid d_5-phenol

This previous study[28] also provided a series of simulations of the effect of "ring-flips," 180º rotations of the ring about the O-C bond at rates varying from $k = 10^3$ s^{-1} (slow exchange) to $k = 10^8$ s^{-1} (fast exchange). The appearance of the spectrum changes in a characteristic way that places more intensity in the center of the spectrum relative to the horns, and removes intensity beyond the horns (seen as weak shoulders in Fig. 42). There appears to be a weak doublet with a splitting of 31.4 kHz in Figure 42, which interestingly resembles the splitting in the central portion of the theoretical simulations for phenol undergoing fast 180º ring flips (a similar small central splitting was also observed in low-temperature spectra of the epoxy primer exposed to the solvent mixture or 10 minutes, discussed below). In a pure compound one with molecules in the slow-exchange limit (i.e. not flipping), one would not expect to have a small subset undergoing

flips in the fast-exchange limit. However, it is conceivable that impurities in the lattice might lead to a portion of the sample experiencing such flips.

The simulations of the effects of ring flips in phenol[28] are of value in interpreting the ^{2}H results we have obtained for the MIL-PRF-23377 epoxy primer sample exposed to d_5-PhOH/EtOH (3.115/1.0). Figure 43 shows the ^{2}H quadrupolar-echo NMR spectra of the exposed sample for four different tau values in the echo sequence.

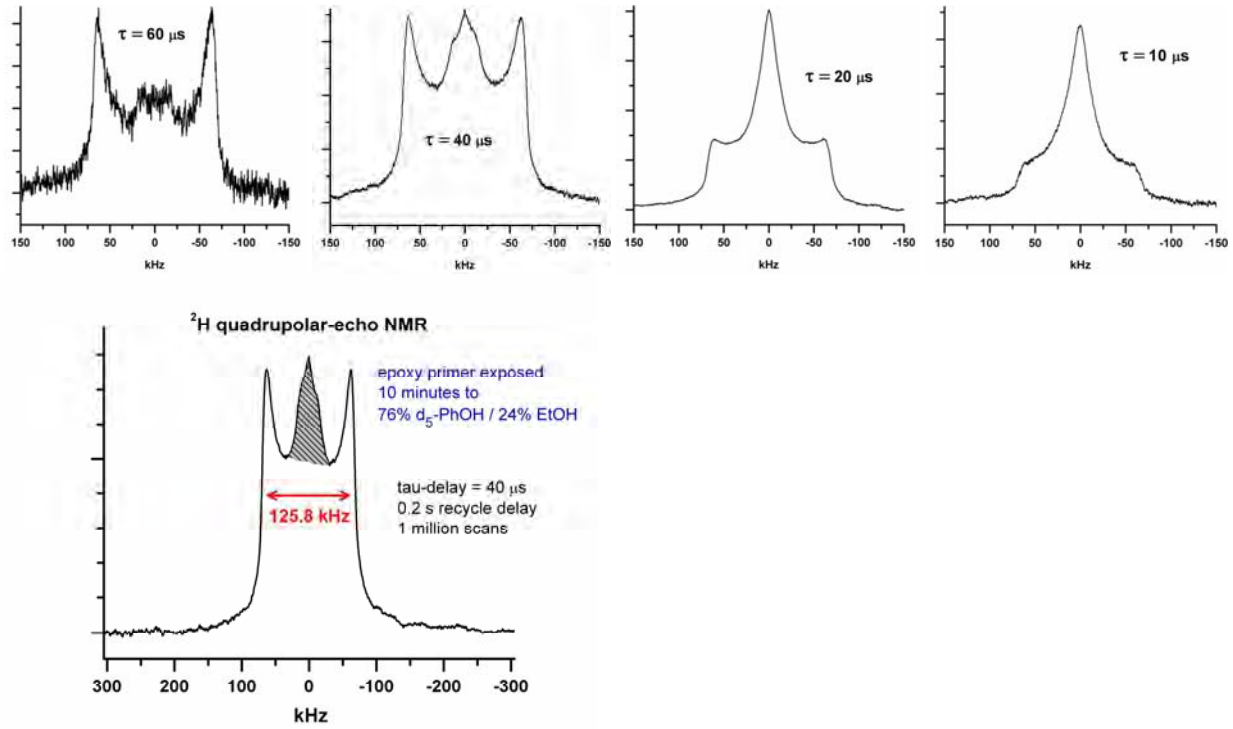

Figure 43: ^{2}H quadrupolar-echo NMR spectra at 24 ° C of MIL-PRF-23377 epoxy primer exposed to d_5-PhOH/EtOH (3.115/1.0) for 10 minutes, at four different echo times tau as indicated. The differing signal to noise ratios reflect differences in the number of scans acquired. The recycle delay was 0.2 s and exponential apodization (linebroadening) was 300 Hz. A wider plot of the τ = 40 μs spectrum is also depicted with a shaded region arising from the more mobile second component having a shorter T_2.

The shortest echo time (10 μs) yields a spectrum having a peaked tent-like appearance, but as the echo time increases, the central peak is seen to gradually disappear, leaving primarily a pattern very similar to that seen for bulk solid d_5-phenol (Figure 42), with a splitting between the horns of ca. 139 kHz. We thus conclude that there are at least two types of phenol molecules in the epoxy sample having very different T_2 values. The one with the longer T_2 is rather rigid and does not undergo 180° ring flips or any other substantial motion at a rate faster than about 10^4 s^{-1},

based on theoretical simulations.[28] The other type of phenol molecule has a much shorter T_2 as a result of restricted motion at a rate fast compared to the static quadrupole coupling constant, greater than perhaps 10^6 s^{-1}. This motion is not simply a 180º ring flip, since the theoretical spectra for such a process are quite different from what is observed.[28] The HHLW of the second component is of the order of 20 kHz, which if it were due to a homogenously broadened ^2H spectrum, as was observed for CD_2Cl_2 in MIL-DTL-53039 above, would correspond to a T_2 value of ca. 16 μs. The relative proportions of the two types are difficult to determine, but from the 10 μs spectrum the mobile component appears to be dominant.

In order to obtain more information about the motional processes taking place, variable temperature quadrupolar-echo spectra were acquired and are shown in Figure 44.

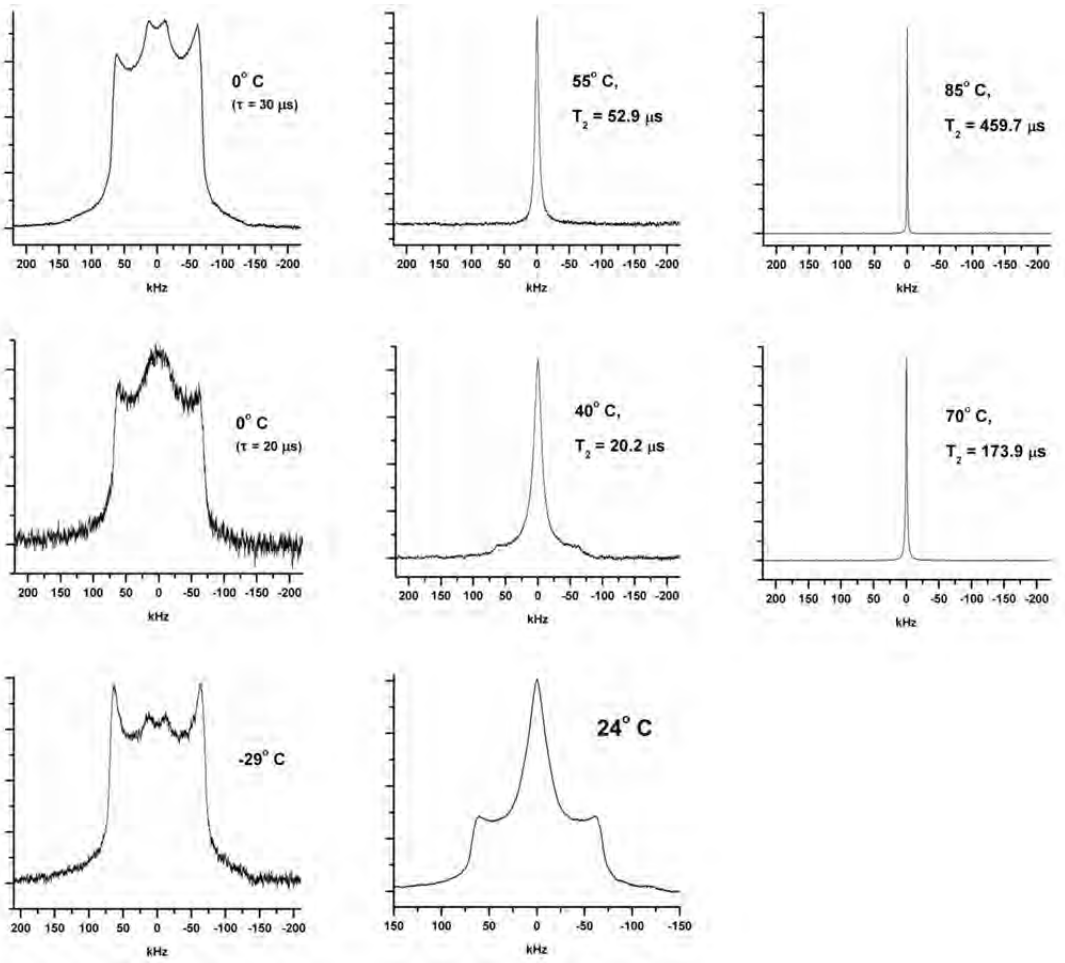

Figure 44: ^2H quadrupolar-echo NMR spectra of MIL-PRF-23377 epoxy primer exposed to d_5-PhOH/EtOH (3.115/1.0) for 10 minutes, at different temperatures. The recycle delay was 0.2 s, exponential apodization (linebroadening) was 300 Hz, and τ = 20 μs except as noted.

At the lowest temperature of -29º C the spectrum obtained with the echo time τ = 20 μs (a shorter time was not used because of the indication of some artifacts in the previous τ = 10 μs spectrum) showed a broad pattern characteristic of rigid phenol molecules not undergoing ring flips, with a splitting of the horns of 127.4 kHz. Changing the recycle delay from 0.2 s to 4 s did not change the appearance of the spectrum (data not shown). Curiously, a small central portion of the powder pattern is seen, with a splitting of 25.1 kHz, and resembling that seen for the bulk sample. As discussed above for that sample, it suggests that some fraction of the phenol molecules may be undergoing 180º ring flips. The spectrum at 24º C was discussed above (from Figure 42).

At 40º C, in addition to a broad pattern with a splitting of 125.2 kHz that may reflect fairly rigid phenol molecules not undergoing ring flips (despite being just below the melting point of the bulk solid), there is a much sharper single central peak with a HHLW of 15.1 kHz. The spectrum changes as the echo delay τ is increased from 20 to 80 μs (data not shown), at which point no signal is observable. The T_2 obtained from a single-exponential fit is shown on the plot, and $1/(\pi T_2)$ = 15.8 kHz, which is even slightly above the observed HHLW and indicates homogeneous broadening by T_2 relaxation as the source of the entire linewidth observed. Further sharpening is observed at 55º C, where as the echo delay τ is increased from 20 to 100 μs a decay with T_2 = 52.9 μs can be observed. The corresponding predicted homogeneous HHLW is 6.02 kHz, which is just slightly less than the observed HHLW of 6.31 kHz. Further sharpening is observed at 70º C, where as the echo delay τ is increased from 20 to 380 μs a longer decay with longer T_2 = 173.9 μs can be observed. Again, the predicted HHLW of 1.83 kHz is very close to the observed HHLW of 1.85 kHz. Yet further sharpening is observed at 85º C, where as the echo delay τ is increased from 20 to 580 μs a still longer T_2 of 459.7 μs is obtained, corresponding to a predicted HHLW of 0.69 kHz to compare with the experimental HHLW of 0.77 kHz.

The supposition that the central peak in these spectra at 40º C and above is due to phenol that has attacked and is covalently attached to the epoxy polymer chain would predict that that the peak would become sharper at higher temperatures due to increased segmental dynamics, as is observed, due to a combination of a decreased residual quadrupolar interaction as the phenol moiety experiences a wider range of orientations as well as a longer T_2 value due to increased

rates of motion. (Below 40 °C such a covalently bound phenol group would become increasingly solid like.) Single-pulse ^{1}H NMR spectra were obtained on this sample at the various temperatures using the decoupling channel of the double-resonance probe. While not free of proton background signals, a marked decrease in HHLW was observed as the temperature increased from -29º C (~42 kHz) to 0º C (~33 kHz) to 40º C (ca. 11 kHz) to 55º C (ca. 8 kHz) to 85º C (ca. 7 kHz). This reduction in HHLW with increasing temperature compares well to the ^{1}H HHLW vs. temperature results in Figure 40 for the same polymer exposed for 10 minutes to the undeuterated solvent mixture, which had a very similar solvent uptake. The slightly greater reduction in HHLW observed for that sample in Figure 40 may have to do with the contributions of a sharper peak from the protonated phenol to the overall signal.

While the ^{2}H NMR linewidth narrowing at higher temperatures thus parallels in a crude sense the ^{1}H NMR linewidths, a direct comparison is not meaningful for several reasons. For one, chemical shift differences contribute significantly to the ^{1}H results, especially the 7 kHz (14 ppm) linewidth observed at 85º C. Also, even if the phenol group is covalently attached to the polymer, it would have additional degrees of motional averaging of its anisotropic (quadrupolar) interaction compared to the main polymer backbone. This could explain the absence of any quadrupolar splittings due to residual anisotropic interactions in the ^{2}H spectra above 40º C. Any interpretation of the ^{2}H NMR results that excludes this covalent attachment would have to account for the marked increase in T_2 as the temperature is increased from 40º C to 85º C. It is conceivable that strong molecular interactions, most likely involving hydrogen bonding, could take place with groups on the polymer and lead to significant temperature-dependences. It would also be valuable to investigate the T_2 temperature dependence of the molten d_5-phenol phase (whose melting point may differ slightly from that of the normal unlabeled molecule) to see if intermolecular hydrogen bonding might strongly influence the relaxation behavior.

The ^{2}H quadrupolar-echo NMR spectra of the MIL-PRF-23377 epoxy primer sample exposed to d_5-PhOH/EtOH for 2 hours showed narrower peaks at comparable temperatures than those observed in the sample exposed for only 10 minutes (see Figures 44 and 45). At -7º C there is a ca. 6 kHz broad peak and a sharper peak with HHLW of ca. 260 Hz seen with an echo delay time τ of 20 μs, the latter being emphasized upon increasing τ from 20 to 400 μs.

At 8º C the HHLW is 1.9 kHz with τ of 20 μs, but a τ of 100 μs clearly shows the bimodal character, with a sharper component becoming more apparent. Further increasing the τ to 400 μs yields only the longer T_2 sharper component, whose HHLW is 244 Hz.

At 24º C with a τ of 20 μs a peak with a HHLW of 640 Hz is observed. It appears that the bimodal character of the lower-temperature spectra is being made less conspicuous by the broad component becoming sharper at higher temperature. This interpretation is supported by the observed decrease in HHLW from 640 Hz to 530 Hz as τ is increased from 20 μs to 420 μs (data not shown). Going to 40º C and using a τ of 100 μs gave the sharpest peak in this series, with a HHLW of 400 Hz.

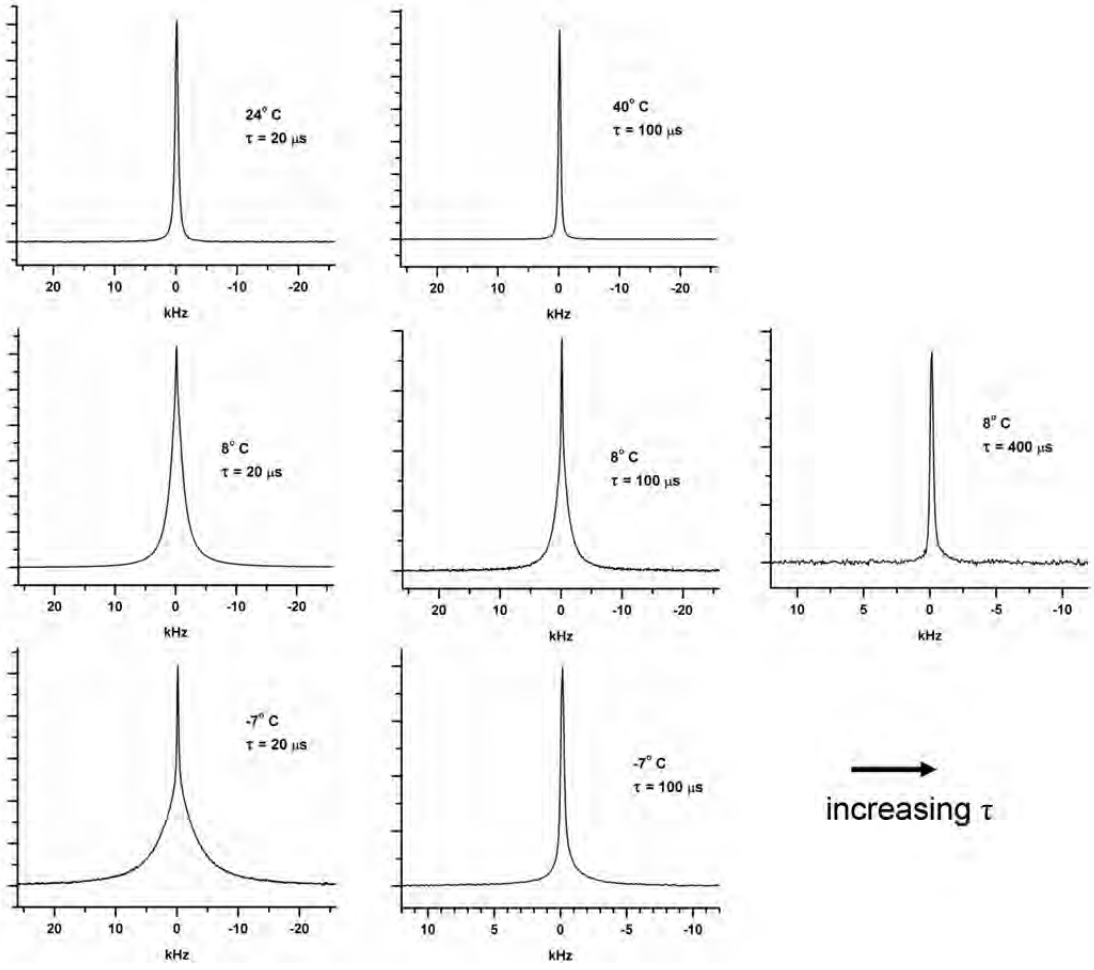

Figure 45: ^{2}H quadrupolar-echo NMR spectra at 24 º C of MIL-PRF-23377 epoxy primer exposed to d_5-PhOH/EtOH (3.115/1.0) for 2 hours, at four different temperatures and different echo times tau as indicated. The recycle delay was 0.2 s and exponential apodization (linebroadening) was 20 Hz. Note the expanded scale on two of the spectra at longer tau values.

As with the results for CD_2Cl_2 discussed above, there are two possible sources of broadening of the ^2H NMR peaks. One is the presence of residual (partially-averaged) quadrupole coupling constants due to partial orientation of the molecules. Such orientation could result from molecules constrained in a non-spherical "cavity" within the swollen polymer, as well as from molecules that loosely bind in preferred orientations to groups in the polymer; distributions of such residual quadrupole couplings would be likely. The second possible source of broadening is purely due to transverse relaxation of an isotropically tumbling molecule whose rotational correlation time is shortened over that in the pure solvent due to the polymer matrix it finds itself inside. Weak interactions with groups on the polymer could also play a role in slowing down the tumbling rate.

In order to test which of these possibilities are operative, we carried out measurements of the transverse relaxation time T_2 in the sample at 24º C using two different types of echo pulse sequences, as shown in Figure 46. The quadrupolar-echo sequence yielded a single-exponential decay constant T_2 of 587.3 μs. This sequence is highly effective in refocusing ^2H nuclei with residual quadrupole couplings, as it is also for ^1H-^1H dipolar couplings betweens isolated pairs of proton nuclei (the sequence in fact was originally developed for the latter case, and is called a "solid echo" pulse sequence when applied there). However, it is not designed to refocus ^2H nuclei lacking residual quadrupole couplings. In contrast, the Hahn echo sequence (90º-τ-180º-τ-Acquire) is designed to refocus nuclei in the latter case, but may also refocus nuclei with suitably small residual quadrupole couplings. This may explain the systematic deviation from a good fit to a single-exponential for the Hahn-echo data in Figure 46. A biexponential however produces an excellent fit, with 89.3% of the signal having a T_2 of 573.0 μs and 10.7% having a much longer T_2 of 2996.2 μs. We note that the shorter T_2 value agrees well with that measured from the quadrupolar-echo data, and we thus attribute it to nuclei having small residual quadrupole couplings. The T_2 component of nearly 3 ms we can therefore attribute to more nuclei lacking such residual couplings and behaving as an isotropic liquid with, however, slower rotational tumbling than that of phenol in a normal solvent. We note that a more complicated procedure involving linear combinations of the signals from three pulse sequences of the solid echo and Hahn echo type have been used to cleanly separate the two types of nuclei in the case of $^!H$ in polymer networks having residual dipolar couplings,[29] and related approaches were earlier

applied to ^{2}H NMR.[30] Such techniques could prove valuable in further NMR studies of these solvent/paint systems.

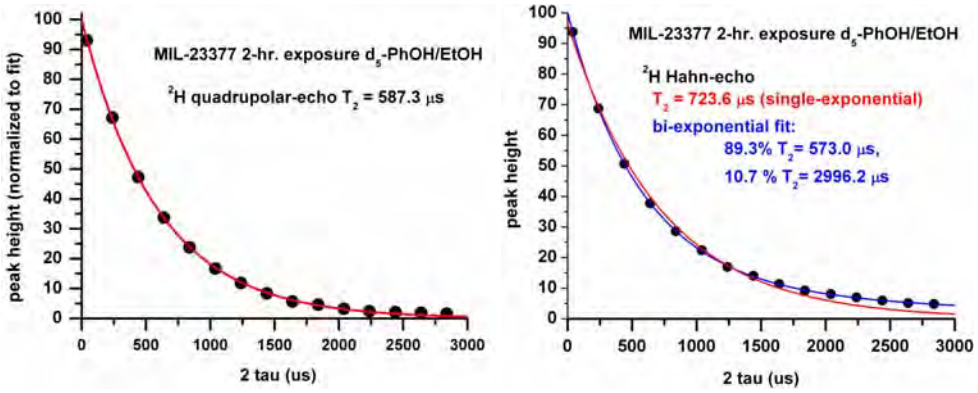

Figure 46: ^{2}H decay times at 24º C of MIL-PRF-23377 epoxy primer exposed 2 hours to d_5-PhOH/EtOH, as measured by two different echo pulse sequences (see text). The single-exponential fit on the right is systematically lower than the experimental data points, unlike the biexponential fit.

Interestingly, the shorter T_2 of 573 μs measured as the major component of the biexponential analysis of the Hahn echo results would predict a HHLW of a Lorentzian peak of 555 Hz, which is just slightly below the observed 590 Hz linewidth. Magnetic susceptibility differences and magnetic field inhomogeneities could easily account for the 35 Hz difference. Thus, for the majority of the phenol molecules in this sample it appears that the residual quadrupolar couplings, although appearing to be responsible for the signal observed in the quadrupolar-echo sequence, must be rather small, and the majority of the peak broadening observed is due solely to relaxation.

We can now try to consolidate this interpretation of the T_2 data with the temperature dependence of the spectra shown in Figure 45. The spectra obtained with the shortest τ value of 20 μs are the most quantitative, in the sense of representing best the relative proportions of broad and sharp components of the spectra. The -7º C spectrum clearly shows that the broad component dominates the sharper component, and is qualitatively consistent with the 89.3% fraction having the shorter T_2 in the biexponential analysis of the 24º C data above. The narrowing of the broader component observed as the temperature is raised to 8º C thus strongly suggests that the d_5-phenol group is covalently bonded to the polymer, the narrowing arising from increased segmental motion at higher temperature. The non-Lorentzian appearance of the broad

component indicates that it does not arise from an isotropically-tumbling free molecule, even one with a lengthened rotational correlation time. At 24º C and higher the bimodal character is difficult to see because the broad component attributed to covalently-bound phenol sharpens so significantly. If this interpretation is correct, it appears that most of the phenol in the epoxy sample exposed for 2 hours, with its 124.5% weight gain, may be covalently bonded to the polymer. This would indicate a very extensive reaction, presumably of the phenolate anion with nucleophilic sites either on the polyoxymethylene backbone or on side groups and cross-linking groups as well.

Before discussing some ^{1}H NMR results for this sample, we want to mention the sole literature example we are aware of that studied the motions of d_5-phenol in a polymer by ^{2}H NMR. In a study of d_5-phenol absorbed from CCl_4 solution over 2 days by a rod of Nylon 6, a Lorentzian peak with a HHLW of about 2 kHz was observed, that broadened upon tensile deformation due to partial ordering.[20] The results cannot be compared with ours, except to note a similar reduction in linewidths from the static value due to dynamics.

A limited number of ^{1}H NMR spectra of this sample were obtained at the same time as the ^{2}H experiments were performed. Figure 47 shows ^{1}H single-pulse NMR spectra of this epoxy sample exposed to d_5-PhOH/EtOH for 2 hours obtained at several temperatures while the sample was in the deuterium probe, by using the ^{1}H double-resonance channel. Although a substantial proton background signal was observed from this probe (unlike the proton probe used for the detailed studies above), quantitation indicated that the signals observed were dominated by the sample. Also, although chemical-shift referencing to a sample of methanol had been carried out earlier, the slow magnet field drift over the two-week interval will introduce a small error on the order of less than a ppm into the chemical shift positions (but not the measured splittings depicted in the figure). The presence of two partially-resolved and fairly sharp ^{1}H NMR peaks over the temperature range -7º C to 40º C is the most obvious feature of the spectra. The separation between the peaks varies in a non-monotonic way with temperature, due mainly to chemical shift changes of the left peak. (data not shown). The assignment of these two peaks to either solvent or polymer groups is not clear at this point. Ethanol itself shows methyl and methylene peaks at 0.96-1.25 ppm and 3.34-3.72 ppm in various organic solvents, with a separation of ca. 2.4 ppm.[31] The chemical shift of the OH peak of methanol in different solvents

varies widely depending upon the degree of hydrogen bonding, and can range from at least 1.3 to 4.6 ppm.[31] (Higher temperatures generally disrupt hydrogen bonding and produce low-frequency shifts (to the right in the spectrum). The apparent absence of two peaks in a 3:2 ratio from the methyl and methylene protons (small J-couplings would not be resolved) that have an invariant chemical shift separation is rather puzzling. Ethanol, even allowing for some evaporation, should be a significant constituent in the sample: 13.5%, based on the uptake, and assuming that the 3.115/1 ratio of the d_5-phenol/ethanol solvent mixture is unchanged in the swollen polymer. It is possible that this latter assumption is not met, i.e. the proportion of ethanol decreases in the polymer; chemical spectroscopic analysis of extracted solvent would be a useful way to determine if this is the case. The contribution from residual aromatic protons on the phenol ring should be minimal in view of the 98% deuteration level of these protons. Since the phenol OH was not deuterated, it is tempting to suppose that the fairly sharp peak on the left might be due to hydrogen-bonded OH groups, which would have a temperature-dependent shift. The polymer backbone is likely to contribute to the broader peak at the base, which appears to narrow at higher temperatures as expected for increasing segmental dynamics. It is also possible that methyl groups somewhere in the polymer itself give rise to the peak on the right. A more detailed study of the ^{1}H NMR behavior of this system could clear up these ambiguities.

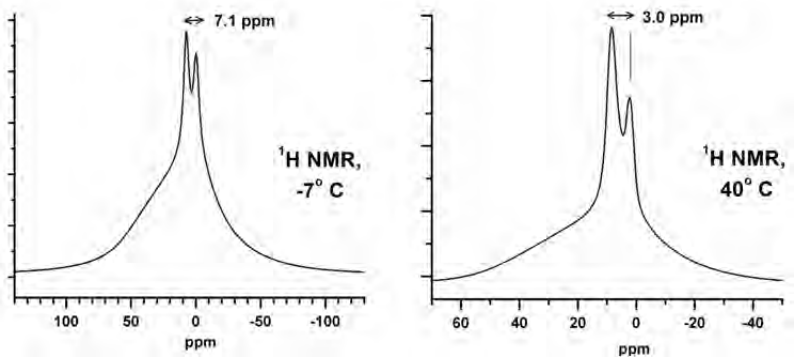

Figure 47: ^{1}H NMR spectra of MIL-PRF-23377 epoxy primer exposed 2 hours to d_5-PhOH/EtOH at two different temperatures.

Conclusions

We report the determination of the mode of action of methylene chloride and phenol in organic solvent based paint strippers. Clear versions of currently in use military coatings were created. The changes in physical and molecular-level properties of these clear coatings as well as the commercial equivalents after exposure to components of the paint stripper including methylene chloride and phenol are reported herein. We characterized the coatings using DSC, TGA, FTIR-ATR, Raman, XPS, and ^{1}H and ^{2}H solid-state NMR. Our results indicate that methylene chloride acts as a facilitator for the other solvents in penetrating the coating but methylene chloride itself is not responsible for coating degradation. ^{1}H NMR results show that methylene chloride solvates the coating and is in close contact with the polymer chains. Raman spectroscopy further confirms that methylene chloride solvates the carbonyl bond to cause dilation. Deuterium NMR confirms this by showing restriction to the tumbling of methylene chloride likely do to some dipole-dipole interaction with the polymer as the solvent's interaction energy is relatively weak. DSC shows significant depression of the glass transition temperature of all the coatings after exposure to solvent mixtures containing phenol, but little change after exposure to methylene chloride. The control mixture containing multiple solvents from the paint stripper caused the greatest coating degradation, suggesting that while phenol is the principal agent in glass transition depression, the other solvents, particularly water, play a significant role. FTIR-ATR and XPS results indicate a hydrolysis reaction occurring, at least at the surface, of samples exposed to methylene chloride/ethanol/water solutions. Nucleophilic attack of the polymer backbone by phenol is suggested by the thermal, vibrational and deuterium NMR spectroscopic data, although unambiguous confirmation of this reaction is still needed. Findings from vibrational spectroscopy have indicated a significant change in the chemical structures as a result of solvent exposure. This change is particular to the solvent mixture used, especially phenol exposure, which causes the greatest difference in the spectra. Solid-state ^{1}H NMR data suggest that the stripper components rapidly exert very significant effects that increase the polymer segmental dynamics in a fashion similar to what takes place in the untreated coatings by heating to much higher temperatures. Deuterium NMR of d_2-MC (CD_2Cl_2) at various temperatures shows that the methylene chloride molecule present in a polyurethane topcoat is not rigid but rather undergoes isotropic rotational tumbling. The rate of tumbling however is orders

of magnitude slower than that in solvents, suggestive of weak interactions with groups on the polymer, perhaps via electric dipoles. The deuterium NMR of an epoxy primer exposed to d_5-phenol/ethanol for different lengths of time reveals a wealth of detailed dynamical information for each sample exposure from changes in the spectral appearance and the T_2 as a function of temperature. Molecular dynamics behavior ranging from rigid phenyl rings on the phenol, to 180º ring flips, to anisotropic motions of varying amplitudes, to completely isotropic motions, are observed. The results suggest a model in which phenol inserts itself into the polymer backbone via nucleophilic attack. FTIR analysis does show phenol within exposed samples well after drying, indicating that the molecule is bound to the polymer resin either via chemical reaction or steric hindrance. The deuterium NMR results are also consistent with covalent attachment. The data thus far suggest that there is a combination of chemical reaction of the most vulnerable linkages within the coating as well as destruction due to swelling beyond the capability of the polymer making up the coating. The possibility of mechanically-induced covalent bond breakage[32] due to swelling forces needs to be considered as does the possibility of chemical attack of the polymer backbone as our observations tend to support these ideas.

Literature Cited

Meetings/Reports

Watson, K.E.; Wynne, J.H. Yesinowski, J.P.; Han, Y.; Young, C.N.; Clayton, C.R. “Mode of action of chemical paint strippers in removing robust polymeric coatings” 242nd ACS National Meeting and Exposition, August 31, 2011, Denver, CO, poster 14553.

Watson, K.E.; Wynne, J.H. Yesinowski, J.P.; Young, C.N.; Clayton, C.R. “Role of Methylene Chloride and Phenol in Chemical Paint Strippers” 41st Annual ACS Mid-Atlantic Regional Meeting, April 11, 2010; paper 212.

Wynne, J.H.; Watson, K.E.; Yesinowski, J.P.; Young, C.N.; Clayton, C.R.; Nesteruk, N.; Kelley, J.; Braswell, T. "Interim Report on Scientific Basis for Paint Stripping; Mechanism of Methylene Chloride Based Paint Removers" NRL Memorandum Report # NRL/MR/6120-10-9303.

Watson, K.E.; Wynne, J.H.; Lundin, J.G.; Yesinowski, J.P. "Novel Environmentally Friendly Approach to Paint Strippers Based in Interfacial Mechanistic Studies" 240th Annual ACS National Meeting, August 25, 2010; Boston, MA, poster 281.

Watson, K.E.; Wynne, J.H.; Yesinowski, J.P. "Progress Toward Understanding the Mechanism of Action in Methylene Chloride/Phenol Based Paint Strippers" 2010 Partners in Environmental Technology Technical Symposium & Workshop, December 1, 2010, Washington, DC, poster 50, abstract #42.

Young, C. N.; Clayton, C.R. “Spectroscopic analysis of the effects of methylene chloride- and phenol-based paint stripping solvent exposure on model coating systems” 2010 Partners in Environmental Technology Technical Symposium & Workshop, December 1, 2010, Washington, DC, poster 69, abstract #313

Journals

1. J. Durkee, *Metal Finishing*, 2009, **107**, 49.
2. T. Wollbrinck, *Journal of the American Institute for Conservation*, 1993, **32**, 43.
3. S. Spring, *Metal Finishing*, 1959, **57**, 63.
4. V. Del Nero, C. Siat, M. J. Marti, J. M. Aubry, J. P. Lallier, N. Dupuy and J. P. Huvenne, in *The proceedings of the 53rd international meeting of physical chemistry: Organic coatings*, AIP, Paris, France, 1996, pp. 469.
5. K. R. Stone and J. Springer Jnr, *Environmental Progress*, 1995, **14**, 261.
6. S. G. Croll, *Journal of Coatings Technology Research*, 2009, **7**, 49.
7. V. P. Volkov, K. V. Nel'son, E. N. Sotnikova, N. P. Apukhtina and L. I. Potepun, *Journal of Applied Spectroscopy*, 1982, **36**, 557.
8. G. L. Marshall and J. A. Lander, *Eur. Polym. J.*, 1985, **21**, 959.
9. R. A. Scott, B. A. Cowans and N. A. Peppas, *Journal of Polymer Science Part B-Polymer Physics*, 1999, **37**, 1953.
10. W. T. Ford, M. Periyasamy and H. O. Spivey, *Macromolecules*, 1984, **17**, 2881.
11. L. Calucci, C. Forte and E. Ranucci, *Biomacromolecules*, 2007, **8**, 2936.
12. I. Devotta, V. Premnath, M. V. Badiger, P. R. Rajamohanan, S. Ganapathy and R. A. Mashelkar, *Macromolecules*, 1994, **27**, 532.
13. R. A. Orza, P. Magusin, V. M. Litvinov, M. van Duin and M. A. J. Michels, *Macromolecules*, 2007, **40**, 8999.
14. K. Ogino and H. Sato, *J. Appl. Polym. Sci.*, 1995, **58**, 1015.
15. S. Schlick, Z. Gao, S. Matsukawa, I. Ando, E. Fead and G. Rossi, *Macromolecules*, 1998, **31**, 8124.
16. L. W. Jelinski, J. J. Dumais, A. L. Cholli, T. S. Ellis and F. E. Karasz, *Macromolecules*, 1985, **18**, 1091.
17. L. S. Loo, R. E. Cohen and K. K. Gleason, *Polymer*, 2000, **41**, 7699.
18. B. Deloche and E. T. Samulski, *Macromolecules*, 1981, **14**, 575.
19. P. T. Callaghan and E. T. Samulski, *Macromolecules*, 2003, **36**, 724.
20. L. S. Loo, R. E. Cohen and K. K. Gleason, *Macromolecules*, 1999, **32**, 4359.
21. Z. Veksli and W. G. Miller, *Macromolecules*, 1975, **8**, 248.
22. A. Guyot, A. Revillon, M. Camps, J. P. Montheard and B. Catoire, *Polym. Bull.*, 1990, **23**, 419.
23. S. L. Regen, *J. Am. Chem. Soc.*, 1974, **96**, 5275.
24. S. L. Regen, *J. Am. Chem. Soc.*, 1975, **97**, 3108.
25. S. L. Regen, *Macromolecules*, 1975, **8**, 689.
26. Image from Cytec webpage, www.cytec.com
27. J. P. Yesinowski, *J. Am. Chem. Soc.*, 1981, **103**, 6266.
28. M. A. Janusa, X. Wu, F. K. Cartledge and L. G. Butler, *Environmental Science & Technology*, 1993, **27**, 1426.
29. P. T. Callaghan and E. T. Samulski, *Macromolecules*, 1997, **30**, 113.

30. J. Collignon, H. Sillescu and H. W. Spiess, *Colloid & Polymer Science*, 1981, **259**, 220.
31. H. E. Gottlieb, V. Kotlyar and A. Nudelman, *J. Org. Chem.*, 1997, **62**, 7512.
32. S. S. Sheiko, F. C. Sun, A. Randall, D. Shirvanyants, M. Rubinstein, H. Lee and K. Matyjaszewski, *Nature*, 2006, **440**, 191.